NASA CONTRACTOR REPORT

NASA CR-1765

INDUCTION PLASMA NOZZLE TESTS

by John W. Poole and Charles E. Vogel

Prepared by
TAFA DIVISION
HUMPHREYS CORPORATION
Concord, N. H. 03301
for Lewis Research Center

NATIONAL AERONAUTICS AND SPACE ADMINISTRATION • WASHINGTON, D. C. • APRIL 1971

1. Report No.	2. Government Accession No.	3. Recipient's Catalog No.
NASA CR-1765		

4. Title and Subtitle	5. Report Date
INDUCTION PLASMA NOZZLE TESTS	April 1971
	6. Performing Organization Code

7. Author(s)	8. Performing Organization Report No.
John W. Poole and Charles E. Vogel	None
	10. Work Unit No.

9. Performing Organization Name and Address	11. Contract or Grant No.
TAFA Division Humphreys Corporation Concord, New Hampshire 03301	NAS 3-13227
	13. Type of Report and Period Covered
12. Sponsoring Agency Name and Address	Contractor Report
National Aeronautics and Space Administration Washington, D. C. 20546	14. Sponsoring Agency Code

15. Supplementary Notes

16. Abstract

An experimental program was conducted to establish induction coupled arc plasma systems with high exit gas enthalpies which could be used to study various nozzle designs. The objective of this work was closer simulation of the nozzle environment expected in the Gas Core Nuclear Rocket. Air plasmas with enthalpies up to 13,000 Btu/lb were developed and evaluation of transpiration cooled and seeded-transpiration cooled nozzles was conducted. It was shown that transpiration cooling reduces the thermal load to the nozzle and the seeded-transpiration cooling further reduces the thermal load.

17. Key Words (Suggested by Author(s))	18. Distribution Statement
Induction plasma heating Propulsion systems Gas concentrations	Unclassified - unlimited

19. Security Classif. (of this report)	20. Security Classif. (of this page)	21. No. of Pages	22. Price*
Unclassified	Unclassified	48	$3.00

*For sale by the National Technical Information Service, Springfield, Virginia 22151

FOREWORD

The work described in this report was done by the TAFA Division of the Humphreys Corporation under NASA contract NAS 3-13227. Mr. Chester D. Lanzo of the Lewis Research Center Nuclear Systems Division was the NASA Project Manager.

TABLE OF CONTENTS

INDUCTION PLASMA NOZZLE TESTS

By John W. Poole and Charles E. Vogel

SUMMARY

An experimental program was conducted with the goal of producing high pressure, high enthalpy arc plasmas which could be used to study various nozzle cooling techniques. This work was directed toward providing experimental input into the design of the nozzle of the Gas Core Nuclear Rocket which will have to withstand extremely high thermal loads.

Initial studies were directed toward obtaining induction plasma torch operations which produced high enthalpy environments in their exhaust stream. While hydrogen gas would be expected to yield the highest enthalpies, air operation was found to be superior because of the operating characteristics and maximum power limitations of the power supplies available for this work.

Having established the maximum enthalpy environment (13,000 Btu/lb air), testing of various nozzle cooling techniques was commenced. While a dramatic demonstration of nozzle failure in one case and no failure at the same operating condition with transpirant cooling and/or seeding was not achieved due to power limitations, it was possible to show changes in the heat flux being absorbed by the nozzle walls. When a transpiration cooled section was used ahead of the nozzle, the heat flux in the nozzle was reduced as a function of transpirant flow. Reductions in heat flux up to 25% were experienced with transpiration cooling of 22% of the total torch gas flow. The addition of fine particle seeding to the nozzle coolant flow further reduced (up to 15%) the thermal loading on the nozzle walls. These results are encouraging toward the goal of designing a nozzle which can withstand the tremendous heat fluxes (100 Btu/in^2 sec) expected to be encountered in the Gas Core Nuclear Rocket.

INTRODUCTION

The nozzle of the Gas Core Nuclear Rocket will be subjected to extremely high heat fluxes, and conventional cooling techniques are not expected to

provide adequate protection. Two design principles proposed for this application are transpiration cooling and seeded-coolant flow. This report describes experimental work conducted to show the effect of these design principles on the nozzle of an induction plasma torch. This work represents only the initial testing of these design principles using an induction torch capable of producing a high enthalpy plasma.

APPARATUS AND PROCEDURE

This program involved using existing and modified high frequency generating systems. All systems used were calorimetrically instrumented in order that a baseline of performance could be established and so that performance could be completely monitored. The system used for most of this work consisted of a conventional 190 kW dc plate power TAFA induction plasma system (12,700 volts, 15 amperes dc). The control unit used to operate this system consisted of plasma forming gas flowmeters, power supply controls and meters. All torches tested were manufactured by TAFA.

All experimental procedures were similar to those reported previously[1] relative to heat balance techniques and estimation of plasma enthalpies by calorimetry.

SELECTION OF HEAT SOURCE

The development of a high powered torch was required in this program in order to present sufficiently high heat fluxes to a nozzle to discriminate between various cooling techniques. Initial efforts in the program were directed toward developing hydrogen operation since the goal of this program was to simulate the operation of the Gas Core Nuclear Rocket. Four approaches to the attainment of high pressure, high enthalpy operation were investigated. It was intended to scope each of these approaches with a limited number of experiments to determine what appeared most feasible and then to pursue the most promising in greather depth. First, attempts were made to operate a smaller torch than previously used.[2] By reducing the torch diameter and operating at maximum power, it was expected that the efficiency of the induction coupling would be improved since previous work had shown the hydrogen plasma to be extremely small in diameter. Second, an easily ionized core material was

introduced into a standard torch. It had been demonstrated in previous work that the introduction of an easily ionized material into the core of the plasma allowed high flows of hydrogen gas through the torch.[2,3] The third approach was the use of induction coupling to augment the energy in a plasma flow generated from a dc arc. Last was a continuation of the standard torch development using an improved segmented wall. This was designed to allow higher power operation while protecting the quartz tube which contains the plasma. Each of these approaches will be discussed separately in the following pages.

Small Torch Development

The small torch development program utilized a 0.625" i.d. water cooled, segmented metal wall compared to the 1.1" i.d. unit used in previous high enthalpy hydrogen work.[2] Figure 1 shows a cross section of the torch as designed. This was constructed with a standard TAFA Model 56 torch base with some of the components scaled down. During the earlier program the arc diameter for the 100% hydrogen flow was observed to be approximately 1/4". At the maximum power available (189 kW plate) only about 12% of this power was in the exiting plasma. From this it was concluded that if a small diameter torch were employed, much higher coupling efficiency would take place and therefore more power would be available to the plasma.[2] Improving the load to coil diameter ratio affects the efficiency of inductive heating dramatically when the load is only a few times the reference depth. Of even greater importance for hydrogen operation is the effect that the reflected impedance has on the operating characteristic of the power supply. Figure 2 shows the power distribution as a function of the load to coil ratio. On the basis of this curve, the small diameter torch would produce a 30% increase in power in the plasma as compared to the torch previously run. (The load to coil ratio increased from 0.22 to 0.33.)

Unfortunately, it was impossible to ignite this torch. As is characteristic with all induction plasma torches, the ignition must take place with argon gas in the torch. After many attempts it was concluded that the argon ignition arc diameter was larger than the available space in this small torch causing the arc to short out to the walls preventing successful operation. At this time success was being achieved in concurrent developments using easily ionized core material and the augmented dc plasma, thus the small torch work was terminated.

Solid-Feed Operation

During the early phases of the permeable wall torch program,[3] considerable work was done investigating the possibility of operating torches with vapors of various metals and salts as the plasma core material. Several very interesting test series were conducted which demonstrated that a very stable plasma could be retained within a quartz envelope at higher powers and higher gas flow rates than previously had been possible. Likewise previous work[2] had shown that high hydrogen flows could be introduced in a torch if an easily ionized core were maintained. This suggested the possibility of using this technique to produce high powered, high flow hydrogen operation. Prior efforts to operate on hydrogen had revealed that a major problem seemed to be the ability to couple sufficient power into the plasma to sustain it.

The initial experiments conducted to demonstrate the benefits of vaporized metals or salts incorporated a modified TAFA Model 56 torch in which a small graphite crucible was placed near the base. When hydrogen was utilized a boron nitride crucible replaced the graphite because of the severe hydrogen-graphite reaction. Figure 3 shows the equipment set-up, operation with sodium chloride fed from a crucible, and zinc metal introduced in wire form through a hollow graphite rod. In this crucible a limited charge of sodium chloride could be placed which was to vaporize and form the plasma. Severe ignition difficulties were experienced with this configuration which usually resulted in damage to the torch. When ignition was successfully achieved it was found that the vaporization rate of the sodium chloride could not be adequately controlled for successful sustained operation.

In an attempt to control the rate of sodium chloride feed, an alternate injection technique was utilized which incorporated a variable rate powder feeder. The sodium chloride was introduced from this feeder into the torch through a hollow injection probe. Various positions of the point of injection and feed rate were investigated. It was found that when the feed rate was too high, unstable torch operation was experienced; conversely when the rate was reduced until stable operation was achieved, too little vapor was present to significantly affect the coupling and the attendant increase in hydrogen concentration. Subsequent work conducted (Reference 3) involving solid-feed techniques has shown that this approach is extremely attractive; however, at the time this reported work was conducted insufficient data was available to justify further work.

Induction Augmented DC Operation

Consistent with the technique of coupling to an easily ionized core, several experiments were performed to determine the effect of induction coupling to a dc plasma stream. The argon laminar operating capability of the TAFA Model 51 dc torch was combined with additional components to provide induction augmentation as shown in Figure 4. Part A of this figure shows the equipment setup, Part B the dc operation, Part C the induction operation, and Part D the combined operations. The brightness of the combined induction and dc modes which appears brighter than the superposition of the other two operating modes was clearly observed and measured. The radiation level from the combined operation was 0.115 solar constants as compared to 0.042 and 0.040 for the individual modes of operation.* Thus it is seen that for argon/ operation some benefit could be realized in this approach. It became apparent, however, that while this may be an interesting technical approach, it was not a suitable simulation of the GCNR. Discussion between the Contract Monitor and the contractor concluded in agreement to terminate further exploration of this technique.

Improved Standard Torch Design

The fourth approach investigated was improvement to the design of the TAFA Model 56 torch by the addition of a segmented metal wall and improved water cooling. Several iterations of this design led to a maximum power capability improvement of from 30 to 165 kW (the maximum available at TAFA). This configuration operated equally well on air or on hydrogen/argon mixtures, however, the hydrogen/argon volume ratio was limited to about 55/45 due to electrical matching difficulties with the power supply. As more hydrogen was introduced, the resistivity of the plasma increased and more power was required to operate. It was determined, however, that because of its resistivity, air could be operated at higher enthalpy than this hydrogen/argon mixture and was selected as the standard testing condition.

---

*A Hy-Cal Pyroheliometer Model P-8400-B-01-120 was used to obtain these values.

TRANSPIRATION COOLED NOZZLE DESIGN

The end use of the high powered torch was to test the effectiveness of a transpiration cooled nozzle which has the additional capability of the introduction of seeding material for increased thermal protection. This part of the program included not only the design of a nozzle which incorporated this principle but one in which the heat transfer to the wall could be measured as a function of axial position. This design also necessitated some materials study and selection to produce valid results.

The material selection for the nozzle centered logically around the use of a ceramic or permeable graphite as the transpiration cooled elements. The use of ceramics would have required either the adoption of a fixed geometry which could be purchased or setting up fabrication facilities and entering into a materials development and fabrication program. Since neither of these alternatives was particularly attractive compared to the possible use of graphite, this material was chosen. The selection of a particular graphite was guided by the experience of TAFA and others with porous anodes in dc torches.[4,5] This led to the selection of National Carbon NC 60 as the permeable element. The same material was subsequently used for all of the permeable elements on this program and performed extremely well. The actual design considerations and operational criteria will be covered under the section of this report entitled, "Permeable Element Operation."

A major concern in the design of the nozzle configuration was to provide for the calorimetry necessary to establish the heat transfer rate to the wall of the nozzle as a function of axial position. The possibility of using surface heat flux probes located at various points along the nozzle was considered but rejected because of the very close proximity to the induction coil and its inherent electrical noise generation problem. Experience indicated that no thermocouple measurements could be made accurately enough to provide reliable data and the side heating and permeable wall penetration of water cooled probes made the possibility of their use questionable. Consequently, the possibility of a series of heat flux probes along the nozzle was abandoned in favor of an arrangement as shown in Figure 5.

The key to this design is that the permeable inserts in each of the segments can be replaced with water cooled copper insets for calorimetry data at particular operating points. It was assumed that at identical operating points the permeable sections would be exposed to the same heat distribution as the cooled inserts when they were in place. Several changes were made as

the program proceeded in order to yield optimum data. The two piece cylindrical plenum upstream of the throat was changed to a single conical section and no additional sections were used downstream of the throat insert because the pressure ratios tested expanded the exit gas to atmospheric pressure before leaving the throat insert.

Figure 6 shows the modified Model 56 torch coupled to the first nozzle configuration utilizing two copper inserts. This was used for Runs T1 through T23 which were the development runs made to establish the operating points for the program. Figure 7 shows the second segmented nozzle configuration which included a permeable plenum section for the study of boundary layer cooling and transpiration cooling effects. Figures 8 through 10 show the third, fourth and fifth nozzle configurations. These include provision for seeding flow, and eventually in configuration number five both plenum and throat inserts are transpiration cooled permeable elements with provision for seeding between the elements. Operating experience with these configurations will be covered in later sections of the report.

THRUST SYSTEM DEVELOPMENT

An initial thrust measurement system was designed using a precision load cell* to provide accuracy in detecting small changes in thrust associated with various particle seeding and transpiration flow operating conditions. The system was designed to operate in a vertical position with the torch thrust vector downward and a system error of less than 4% at the thrust levels anticipated. A null balance circuit shown in Figure 11 was developed so that up to a 50 lb. dead load could be electrically nulled out prior to or during a run and small load changes on top of that accurately measured. In the bench calibration of this system it was determined that the readout could determine accurately the addition or subtraction of a 5 gram load on top of a base weight measurement of 30 lbs. Figure 12 shows a photograph of the torch set-up with the load cell supporting the static weight of the torch assembly. This was the configuration used for several completely instrumented runs. Unfortunately, during each of these runs difficulties were experienced with readout due to rf interference.

*Revere Electronics Precision Load Cell Model USP1-.05-A.

This interference was found to be particularly responsive to the plate voltage of the induction power supply and to a lesser degree was influenced by the position of the wiring and readout instrument plus the location of personnel standing in the room. Considerable progress had been made in minimizing this rf interference when a starting arc for the torch shorted through the grounded load cell and burned out one of the strain gauges. Since replacement or repair of the load cell would take some weeks, a mechanical thrust measurement system was constructed which proved to be reliable and accurate and was used throughout the remainder of the program.

Figure 13 is a schematic drawing of the torch and nozzle assembly attached to the power supply by flexible water cooled leads and supported on a lever system with a Fisher precision balance as the readout device. This system was calibrated before each run or set of runs by noting the scale reading corresponding to the loading of different precision gram weights placed on top of the torch. The only problem with this mechanical thrust measurement system was a slight zero shift during some sequences of runs which was believed to have been caused by pressure changes in the cooling water. This zero drift is responsible for some of the scatter on the thrust versus torch chamber pressure graph as shown in Figure 14.

Analysis of Figure 14 for a series of runs using the same nozzle demonstrates the value of the thrust measurements in revealing plugging and erosion of the nozzle throat during a run. Since it can be demonstrated that the thrust is a function of the torch pressure for a given nozzle configuration, any departure from the straight line indicates a change in the nozzle. Plugging which reduced the nozzle area caused the pressure in the torch to increase with some increase in thrust, whereas erosion of the throat enlarged the nozzle requiring additional gas flow to maintain pressure and thereby substantially increased the thrust.

OPERATIONAL AND PROCEDURES PROBLEMS

A listing of all significant runs made in this program is presented as Table I.

As discussed in the section entitled, "Selection of Heat Source," much of the early part of the program was devoted to parallel efforts to accomplish

high pressure, high enthalpy hydrogen operation. It became apparent that roughly a 55/45 volume percent mixture of hydrogen/argon represented the maximum hydrogen exposure that could be generated with the available power supply when using a 0.125" diameter nozzle. Since the nozzle heat transfer rates associated with this operation could not fail the nozzle, considerable effort was devoted to establish a technique to increase the heat transfer to the nozzle. Runs were made with air and with nitrogen and nitrogen-hydrogen mixtures in a search for higher heating rates. Runs T14 to T23 represent the efforts made in this direction. Runs T24 through T28 on air demonstrated the capability of operating the power supply to over 160 kW yielding the highest nozzle heating rates. Consequently, the remaining tests on the nozzle configurations were conducted with an air plasma.

Two other techniques were investigated in an attempt to further increase the heat flux at the nozzle. The first was a suggestion by the NASA/ Lewis Contract Monitor to bleed off the cool boundary layer in front of the nozzle. Runs T73, T74, T75, and T76 are a test sequence which includes a calibration run (T73) and then increasing boundary layer bleed off (T74 and T75). Substantial increase in the heat flux in the throat was observed. Run T75 shows an approximate 50% increase over the T73 base line run, however even with this improvement the average heat flux was only about 7 Btu/in^2 sec. as compared to an estimated 70 Btu/ft^2 sec. required to fail the water cooled components. Tungsten particle feeding was combined with the bleed off in Run T76 to note the reduction in heat transfer to the nozzle during seeding.

A second effort to increase the throat heat flux was to move the nozzle throat closer to the plasma arc zone. This was done by constructing a special insert and nozzle body configuration for the Model 56 torch as shown in Figure 9. This configuration operated well but an increase of only 15% in average heat flux to the nozzle configuration was achieved. Run T83 through T85 are the operating points for this configuration.

An interesting operational problem was noted when the first permeable plenum insert was tested. The plasma flame exiting from the torch had been noted to lean in such a way as to be perpendicular to the plane of the top coil of the inductor rather than parallel to the axis of the torch. (The coils are not wound perpendicular to the axis but at a slight angle.) At high power levels or low gas flows, erosion of the insert was noted at the position closest to the arc. This non-uniformity in gas flow was no doubt existent when the water cooled copper nozzle was in place, however sufficiently high heat fluxes were

not attained to cause failure. Several corrective measures were taken in coil design which improved the symmetry of the plasma sufficiently to permit acceptable testing.

CALCULATION OF THEORETICAL THRUST

As a check to determine the reasonableness of measured nozzle thrust values, two approaches were made to calculating specific numbers. Both approaches utilized the thrust equation in the following form:

$$\mathcal{T} = \frac{w}{g} V_e + P_o \left(1 - \frac{P^*}{P_o}\right) A^*$$

where:

$\mathcal{T}$ = Thrust in pounds

$\dot{w}$ = Mass flow in lbs/sec

g = Acceleration due to gravity: ft/sec^2

V_e = Velocity of exit flow in ft/sec

P_o = Torch chamber pressure in lbs/in^2

P^* = Nozzle throat pressure in lbs/in^2

A^* = Area of nozzle throat in in^2

Measured values for torch pressure and throat area are used in the second section of the equation, so the approaches differ only in the technique used to calculate values for w and V_e. The first approach assumes that the flow through the nozzle consists of two components: a hot core from the torch, and a cooler sheath from the transpiration fluid in the nozzle. It further assumes no mixing of these flows. Appendix A presents a sample calculation utilizing this technique. The second approach is one commonly used by plasma wind tunnel technologists to check heat balance enthalpy. It is

completely independent of heat balance measurements, utilizing only torch chamber pressure, mass flow rate and throat area. A sample calculation using this technique is presented in Appendix B which follows the procedure detailed in Reference 6. Table II compares the measured thrust with the values obtained by these two theoretical approaches. It should be noted that reasonable agreement between experimental and calculated values has been achieved. Figure 14 presents the measured thrust values as a function of torch chamber pressure and nozzle configuration.

TRANSPIRATION COOLANT INFORMATION

Since the operating gas through the plasma torch was air for most of the last 70 test runs, it was decided that air should be used as the transpiration coolant. Nozzle configuration number two shown in Figure 7 was the first to use an air flow for cooling. By varying the flow through the plenum element, it was possible to change the thickness of the cool boundary layer introduced to the throat section. Figure 15 shows two curves of the heat flux to the nozzle section as a function of transpiration coolant flow for this configuration. It will be noted that both curves flatten out at the maximum gas throughput used. It seems reasonable to conclude that at this condition the total heating of the nozzle element is through radiation from the arc column.

It was determined that at flow rates of 1 ft/sec (assuming uniform distribution of flow across the insert) or above, sustained high pressure operation could be achieved with no erosion to the surface of the plenum. The flow through the torch during these runs was at a much higher value of 25 ft/sec. This indicates that with very little transpirant flow as compared to torch flow, it is possible to provide significant protection to the nozzle.

Calculation of the temperature rise necessary in the plenum transpiration coolant to handle a typical radiant heating load of 0.5 Btu/sec yields 1500^{o}F or 850^{o}C. Reference 7 lists 0.7 hours for 6% weight loss on a commercial graphite at 700^{o}C in air. This correlates well with the observation that very little if any erosion took place during most of the test runs with a permeable plenum.

It was found that the same tapered plenum insert could be and was operated for some 20-25 runs without replacement. On the other hand, during

some runs the plenum eroded rather badly on one side of the torch. This is believed to have been caused by the directionality problems in the plasma previously mentioned. It is also possible that the particular graphite pieces used for these plenums were not as uniform as required for this application.

In summary, it was determined that the transpiration cooled elements would operate well over a wide range of coolant flows as long as the plasma flow and flow through the permeable wall were relatively uniform.

SEEDED FLOWS

During the course of the program 22 seeding runs were made with various weight percentages of tungsten and silicon powder as the seed material, or as calibration runs prior to seeding. The intent in introducing the seeding material was to avoid burning out a nozzle insert under an operating condition which otherwise would have produced a burnout. Since sufficient power was not available to demonstrate this situation in this way, the effectiveness of various seeding operations was determined by measuring the change in heat transfer to the throat element as a function of seeding flow.

With one exception the introduction of seeding material substantially reduced the heat transfer to the nozzle. Figure 16 shows the results with tungsten and silicon seeding. The one exception occurred when the seed material was introduced with a high carrier gas flow. This flow of about 25 ft/sec was the same as the axial velocity of the plasma out of the torch and resulted in extreme mixing and turbulence in both the plenum and nozzle sections negating the beneficial effect of the seeding. Later runs at the same powder feeding rate but with the carrier gas introduced at lower rates produced the desired result of reduced heating of the nozzle throat.

It was observed that the seed particles tended to react in the gas stream and deposit on the surface of the nozzle. A recent article by Russian authors[8] about chemical reactions in a plasma environment indicated that a 5 micron tungsten particle would melt in about 10^{-5} seconds in a 5,000°K gas stream. If this is correct, the tungsten seeding particles used in this work would be molten before they reached the throat of the nozzle. This circumstance would not affect the heat transfer rate since if you assume the seeding material oxidized, only about 1/10 Btu/sec would be generated as compared to a total of about 20 Btu/sec in the gas stream.

A second interesting observation related to the accumulation of seed material on the elements of the nozzle. This accumulation was experienced with flows up to 3 ft/sec through the permeable plenum. No higher flow rates were tested because of the possibility of disrupting the flow pattern and increasing the thermal loading on the nozzle as noted above. This seeding material accumulation problem produced partial choking of the nozzle throat during the silicon seeded hydrogen/argon test series indicating that this can be a problem even when the material is not reacting chemically with the gas stream. It is proposed that the effect noted here is caused by particles being projected out of the boundary layer flow and then projected back toward the nozzle surface with sufficient momentum to penetrate the boundary layer.

One of the difficulties relative to the seeded flow runs was the actual size of the particles going through the nozzle. The tungsten powder specification showed the following size distribution by photolometer:

Size Distribution Tungsten Seed

Size in Microns	Weight %
0 - 1	67.7
1 - 2	20.4
2 - 3	8.3
3 - 4	2.6

Observation of a sample of this tungsten powder under a microscope showed considerable tendency for the powder to agglomerate and it is not known whether actual particles or agglomerates were injected into the gas stream. The silicon powder was specified as -200 mesh (74 microns), however a screen analysis showed that approximately 70% was -325 mesh (44 microns). Microscopic examination confirmed the screen analysis and revealed that there was little tendency for this powder to agglomerate. This may well explain the higher radiation absorption of the silicon seeded runs even though the tungsten specification indicated that it was the finer powder and should have had a higher absorption coefficient.

In all, 19 runs were made in series where seeding was the primary goal of the test. Four test series were made with 1 micron tungsten seeded into an air plasma. Two of these showed a decrease in heat transfer to the nozzle of 3-11% when seeding with weight percentages of 0.14 to 0.21% of

the total gas flow and carrier gas flows of 0.094 to 0.141 gram per second. The two test series that showed an increase in heat transfer both involved higher seeding rates (1.0 to 1.8 percent by weight) and higher carrier gas flow rates (0.21 to 0.43 gram per second). One of these showed a 12% increase when operating with 1.1% tungsten seeding at 0.21 grams per second carrier gas flow and a 16% increase when the tungsten seeding was increased to 1.8%. The other test series involved seeding through the permeable disc and it is postulated that partial plugging took place so that the bulk of the powder was being fed through a small number of orifices. This could have produced the increase in heat transfer rate just as high flows caused high heating rates in tests T53 through T57. Also in this series it was noted that the tungsten was oxidizing.

One test series was run with tungsten seeding into an hydrogen/argon plasma. This showed a 4% increase in heat transfer rate with 0.14% tungsten seeding in a 0.141 gram per second carrier stream and no increase in the later run when 0.13% tungsten was being fed in the same carrier gas stream. This effect is close to the discrimination limit of the instrumentation, and may again have been due to powder agglomeration.

Two test series were made with silicon as the seed material, one with air plasma and the other with hydrogen/argon plasma. The run with air plasma produced a 15% decrease in nozzle heat transfer rate with 0.21 gram per second carrier gas stream and 0.1% silicon seed rate. This test was run with the -200 mesh silicon powder in the as received condition. The nozzle showed a considerable accumulation of silicon oxide during this run and in fact the test series was prematurely terminated because of an increase in pressure inside of the torch. Thus part of the 15% decrease in heat transfer rate was undoubtedly due to a thermal insulation layer of silicon.

The silicon seeding run on hydrogen/argon plasma (test series T92-T94) showed a 5 1/2% decrease with 0.48% silicon seeding in a 0.17 gram/sec. carrier gas stream. There was no oxidation phenomena during this run and very little accumulation of silicon was noted on the inner surface of the nozzle. Since the silicon powder is gray there would have been a decrease in heat transfer due to the powder buildup and an increase in heat transfer due to the increased absorption of the surface. Regardless of these affects it can be stated that the silicon seeding, which in this case was with -325 mesh material, did reduce the heat transfer to the nozzle. From an engineering viewpoint adequate data and know-how has been developed to give

confidence that a larger model operating at higher powers can now be constructed to operate with seeding and give a significant reduction in nozzle heat flux.

PERMEABLE ELEMENT OPERATION CHARACTERISTICS

As mentioned earlier, the material used for the permeable plenum insert for Run T29 was a strong graphite with 10-20% open porosity and a very non-homogeneous structure. The burnout of one side of the element during test T29 can be attributed to the poor centering of the plasma flow and possibly on the lack of uniform distribution of the transpired coolant through the element. The shift was then made to National Carbon NC 60 porous graphite. Although this is a poor material from a strength point of view (tensile strength of 200 lb/in^2), it has been found to produce excellent results in this kind of application. Figure 17 shows the pore size distribution for a typical sample of NC 60 and Figure 18 shows a typical gas flow distribution for this material as a function of position on the surface. The material is advertised to have about 48% porosity.

The NC 60 material has been used as the transpiration cooled anode for a period of years by TAFA and others.[4,5] It should be noted and emphasized that in the reports covering the work of Sheer, et al with this particular material it was found that a "good" sample of material produced excellent results and in fact held up for a period of a year with typical laboratory operation on a given torch. However an adjoining piece of the same material could produce sufficiently non-uniform flow so that the anode element was burned out in a matter of minutes. From the variation in permeable element life achieved by all investigators it can be concluded that proper inspection and testing of permeable elements for uniform transpiration flow distribution will be a major design requirement in any operational hardware that depends on transpiration cooling.

It had been intended that the thickness of the permeable elements be varied so that an inverse relationship to the anticipated heating loading at a particular cross section could be developed. In fact it was found that the NC 60 material was so permeable that changes of thickness within the size limitation of the hardware had very little effect on the gas flow. This actually became a problem on the last runs when the pressure distribution across the throat section of the nozzle adversely affected the flow of transpiration

coolant to the converging section of the throat contour. If the pressure behind the permeable plenum was set so that a flow would be maintained through the throat of the nozzle, no gas or perhaps even a reverse flow would be experienced upstream. Conversely if the pressure was set to cause flow at the upstream point, the flow through the throat section was excessive. This indicates that it would be desirable to have a material that is less permeable for this application and preferably one whose permeability is highly dependent on thickness.

CONCLUSIONS

The principle goal of the work conducted in this study to show the effects of various nozzle designs on reducing thermal loading to the nozzles has been successfully demonstrated. While high enthalpy hydrogen operation was not achieved due to power supply limitations, it was possible to conduct satisfactory nozzle screening testing with a high enthalpy air plasma. Specific conclusions are as follows:

1. The addition of a transpiration cooled nozzle significantly reduces the thermal loading on the nozzle wall.

2. The addition of a seeded-transpiration cooled nozzle additionally reduces the thermal loading in the nozzle wall over the transpiration cooling alone.

3. These results confirm the basic design principle of transpiration cooling and support the current nozzle design criterion for the Gas Core Nuclear Rocket.

REFERENCES

1. Thorpe, M. L., "Induction Plasma Heating," NASA CR-1143, August 1968.

2. Thorpe, M.L., and Scammon, L.W., "Induction Plasma Heating High Power, Low Frequency Operation and Pure Hydrogen Heating," NASA CR-1343, August 1969.

3. Vogel, C.E., "Curved Permeable Wall Induction Torch Tests," Final Report on Contract NAS3-13226, August 24, 1970.

4. TAFA Bulletin LP19, "Transpiration Cooled Plasma Torch," January 1969.

5. Sheer, C., Kennedy, J.M., Tschang, P.S., "Effects of Mechanical and Thermal Electrode Properties on the Behavior of the Fluid Transpiration Arc," Aerospace Research Laboratories, ARL 63-150, August 1963.

6. Jorgensen, L.H. and Baum, G.M., "Charts for Equilibrium Flow Properties of Air in Hypervelocity Nozzles," NASA TN D-1333, September 1962. (Chart 14, page 74)

7. "The Industrial Graphite Engineering Handbook," Union Carbide Corporation, New York, New York, 1964.

8. Vurzel, F.B. and Polak, L.S., "Plasma Chemical Technology - The Future of the Chemical Industry," Industrial and Engineering Chemistry, Vol. 62, No. 6, June 1970.

9. Jorgenson, L.H. and Baum, G.M., Chart 8, page 51.

10. Moeckel, W. E. and Weston, K.C., "Composition and Thermodynamic Properties of Air in Chemical Equilibrium," NACA TN 4265, 1958. (Chart 2, page 16)

11. Ibid., Figure 4, page 38.

APPENDIX A

NOZZLE THRUST USING THE DUAL-FLOW CONCEPT

This analysis assumes that the flow out of the plasma torch continues through the nozzle without heat loss and occupies the center part of the throat area, and that the remainder of the throat area is filled with the cool transpiration coolant flow. Applied to the data of Run T46,

Exit enthalpy measured by calorimeter 16.9 Btu/sec

$$\text{Torch weight flow} = \frac{167 \times .0753}{3600} = 3.49 \times 10^{-3} \text{ lb/sec}$$

$$\text{Torch exit enthalpy } h_o = \frac{16.9}{3.49 \times 10^{-3}} = 4830 \text{ Btu/lb}$$

Referring to Figure 19 of this report, this enthalpy corresponds to a weight-flow rate of 9.7 lb/sec-atm-ft^2. Solving for the throat area (h for Hot flow)

$$A_h^* = \frac{\dot{w}}{P_t \times 9.7} = \frac{3.49 \times 10^{-3}}{\frac{40.5}{14.7} \times 9.7} = 1.307 \times 10^{-4} \text{ ft}^2$$

This leaves the difference of $(1.531 - 1.307) \times 10^{-4} = 0.224 \times 10^{-4} \text{ft}^2$ for the cool flow of the boundary layer.

$$\frac{\dot{w}}{P_t A_c^*} = \frac{67 \times .0753}{3600 \times \frac{40.5}{14.7} \times .224 \times 10^{-4}} = 22.7$$

This corresponds to an enthalpy of $h_c = 590$ Btu/lb from Figure 19.

Using Figure 20, and the Mach number of 1.30 as determined from the pressure ratio*

$u_h = 5860$ ft/sec

$u_c = 2640$ ft/sec

*NACA Report No. 1135, "Equations, Tables, and Charts for Compressible Flow," Ames Research Staff, 1953. (Table II)

Thus the two thrust contributions are

$$\mathcal{J}_h = \frac{3.49 \times 10^{-3}}{32.2} \times 5860 = .635 \text{ lb}$$

$$\mathcal{J}_c = \frac{67 \times .0753}{3600 \times 32.2} \times 2640 = .115 \text{ lb}$$

Total .750

Added to the throat pressure thrust contribution of 0.39 lb from Appendix B, the total is 1.14 lb as compared to a measured 1.30 lb.

The remainder of the thrust is contributed by the reduced pressure region upstream of the throat, plus a very small contribution from the exit cone. The uncertainty involved in the flow uniformity through the nozzle is considered to make further refinement of this calculation technique unjustified.

APPENDIX B

NOZZLE THRUST USING SONIC THROAT ANALYSIS

NASA TN D-1333, Charts for Equilibrium Flow Properties of Air in Hypervelocity Nozzles, provides in Chart 14, p. 74 (reproduced as Figure 19 of this report) a plot of throat stagnation enthalpy as a function of weight-flow rate, lb/sec-atm-ft^2. Applying this to the data of Run T46

Weight flow through nozzle

$$\dot{w} = \frac{234 \text{ ft}^3/\text{hr} \times .0753 \text{ lb/ft}^3}{3600 \text{ sec/hr}} = 4.89 \times 10^{-3} \text{ lb/sec}$$

Using Figure 19

$$\frac{\dot{w}}{P_t A^*} = \frac{4.89 \times 10^{-3}}{\frac{40.5}{14.7} \times 1.531 \times 10^{-4}} = 11.6$$

This corresponds to $h^* = 3{,}000$ Btu/lb.

From NACA Report 1135, Supersonic Flow Table II, at

$$\frac{P}{P_t} = \frac{14.7}{40.5} = 0.363, \quad M = 1.30$$

Then from TN D-1333 Chart 8, p. 51 (reproduced as Figure 20 here) at

$h_t = 3{,}000$ Btu/lb and $M = 1.3$, $u = 4{,}700$ ft/sec. This times the mass flow through the nozzle gives a momentum induced thrust of

$$J_m = \frac{4.89 \times 10^{-3} \times 4.7 \times 10^3}{32.2} = 0.71 \text{ lb.}$$

From NASA TN 4265, p. 16 (reproduced as Figure 21 of this report) at $h^* = 3{,}000$ Btu/lb and $P_t = \frac{40.5}{14.7} = 2.75$ atm. the stagnation temperature is 7050°F, and the entropy $S/R = 35.6$.

Now referring to TN 4265, Figure 4 (Figure 22 of this report) at an enthalpy of 3,000 Btu/lb and entropy $S/R = 35.6$

$$\text{dimensionless enthalpy} = \frac{h\mu_o}{RT_o} = \frac{3000 \times 28.96}{1.987 \times 273} = 160$$

$$\gamma = 1.212$$

The thrust contributed by the pressure imbalance at the throat is

$$F_p = P_t \left(1 - \frac{P^*}{P_t}\right) A^* \quad , \quad \frac{P^*}{P_t} = \left(\frac{2}{\gamma+1}\right)^{\frac{\gamma}{\gamma-1}} = .563$$

$$= 40.5\ (.437)\ .0218 = 0.39 \text{ lb.}$$

Thus the momentum and throat pressure thrust components total 1.10 lb, compared to the measured thrust of 1.30 lb. The remainder of the thrust is contributed by the reduced pressure region upstream of the throat, plus a very small contribution from the exit cone. The uncertainty involved in the flow uniformity through the nozzle is considered to make further refinement of this calculation technique unjustified.

TABLE I - SUMMARY OF SELECTED SEGMENTED NOZZLE OPERATING RUNS

Run No.	Plate Power kW	Total Torch Gas Flow SCFH	Gas Enthalpy at Nozzle Entrance Btu/lb	Nozzle Configuration	Transpiration Flow - SCFH	Seeding Rate lb/sec x 10^5	Exhaust Gas Heat Content Btu/sec	Nozzle Heat Flux Btu/in^2-sec A - Plenum B - Throat A	B	Torch Pressure psig	Nozzle Throat Dia. in.	Measured Thrust lbs.
T1 - T13	- Investigation of maximum enthalpy operation on hydrogen/argon mixtures -											
T14 - T18	- As above with hydrogen-nitrogen mixtures -											
T19	124	114(1)	66,000(2)	1	0	0	10.0	1.72	6.4	12	.161	-
T20	130	119(1)	39,000(2)	1	0	0	1.2	1.36	5.8	19	.125	-
T22	101	240(1)	23,800(2)	1	0	0	7.0	.68	2.9	15	.161	-
T23	95	110(1)	64,000(2)	1	0	0	3.8	1.0	3.2	15	.125	-
T24	110	76(3)	10,300	1	0	0	10.0	1.64	4.4	21	.125	1.27
T25	139	76(3)	12,200	1	0	0	10.9	2.20	5.9	23	.125	1.03
T26	152	76(3)	14,700	1	0	0	14.4	2.36	6.3	23	.125	1.08
T27	156	51(3)	17,700	1	0	0	9.5	2.48	6.3	15	.125	.95
T28	165	51(3)	21,900	1	0	0	13.7	2.56	6.5	15	.125	1.02
T29	110	68(3)	10,500	2	132(4)	0	10.6	-	3.7	28	.161	-
T30 - T34	- Low power runs to develop sealing technique to permeable elements -											
T35	119	168(3)	4,800	2	263(3)	0	15.7	-	0.7	35.5	.161	1.62
T36	118	168(3)	5,600	2	184(3)	0	19.3	-	0.53	31	.161	1.56
T37	117	171(3)	5,400	2	107	0	18.7	-	0.65	27	.161	1.40
T38	155	168(3)	8,100	2	107	0	26.8	-	2.1	30	.161	1.52
T39	155	165(3)	8,600	2	188	0	28.7	-	1.2	35	.161	1.71
T40	152	165(3)	7,800	2	265	0	26.5	-	.84	40	.161	1.92
T41	118	167(3)	5,600	2	67	0	20.6	-	1.04	25	.167	1.18
T42	141	284(3)	2,600	2	210	0	16.0	-	.81	50	.167	2.02
T43	155	166(3)	7,200	2	67	0	27.3	-	2.5	28	.167	1.23
T44	155	166(3)	6,900	2	37	0	27.2	-	3.2	26	.167	1.22
T45	119	166(3)	6,000	2	37	0	21.8	-	.91	24	.167	1.10
T46	118	167(3)	4,500	2	67	0	16.0	-	1.20	26	.167	1.30
T47	155	168(3)	7,600	2	66	0	21.5	-	3.2	29	.167	1.52
T48 - T51	- Repeat of above runs with exit calorimeter to refine heat balance measurement -											
T52	154	167(3)	7,500	2	67	0	24.3	-	2.7	32	.161	1.71
T53	156	166(3)	7,700	3(5)	151	0	21.8	1.84	2.1	44	.161	1.68
T54	156	169(3)	7,400	3(5)	154	0	21.8	1.44	2.3	44	.161	1.70
T55	156	169(3)	7,700	3(5)	154	0	22.5	1.28	3.2	44	.161	1.74
T56	156	169(3)	7,800	3(5)	154	0	22.4	2.36	2.3	45	.161	1.79
T57	156	169(3)	7,100	3(5)	154	0	18.8	2.52	2.2	45	.161	1.80
T58	153	167(3)	6,800	3(5)	19 & 19(7)	0	21.4	.63	1.65	42	.161	1.19
T59	153	168(3)	6,900	3(5)	19 & 19(7)	4.8W	21.6	.69	1.87	42	.161	1.27
T60	153	168(3)	6,300	3(5)	19 & 19(7)	7.9W	19.3	.73	1.93	43	.161	1.40
T61	153	168(3)	6,600	3(5)	19 & 19(7)	0	20.7	.67	1.82	43	.161	1.40
T62	151	168(3)	6,600	3(5)	19 & 19(7)	0	21.3	.60	1.63	42	.161	1.57
T63	150	168(3)	6,100	3(5)	19 & 19(7)	0.7Si	19.5	.54	1.39	48	.161	1.60
T65	158	127(3)	7,000	3(6)	45 & 45(7)	0	22.4	.52	1.03	50	.177	1.14
T66	159	127(3)	6,800	3(6)	15 & 75(7)	0	22.5	.53	0.70	48	.177	1.14
T67	159	127(3)	6,900	3(6)	75 & 15(7)	0	22.2	.49	1.43	51	.177	1.25
T68	159	127(3)	6,700	3(6)	23 & 127(7)	0	22.1	.58	0.63	52	.177	1.30
T69	158	126(3)	6,900	3(6)	23 & 23(7)	0	22.5	.44	1.39	44	.177	1.12
T70	155	154(3)	4,400	3(6)	42 & 41(7)	0	12.5	.54	.98	42	.160	1.34
T71	155	154(3)	4,400	3(6)	41 & 41(7)	4.8W	11.5	.86	1.16	45	.160	1.43
T72	155	154(3)	4,400	3(6)	30 & 20(7)	8.4W	10.8	1.09	2.04	35(8)	.160	1.42
T73	160	171(3)	5,800	3(5)	0 & 20(7)	0	15.2	1.52	3.5	37	.188	(9)
T74	160	171(3)	6,100	3(5)	-16 & 20(7)(10)	0	16.1	1.68	3.3	34	.188	(9)
T75	160	188(3)	5,300	3(5)	-22 & 0(7)(10)	0	13.8	1.60	5.3	32	.188	(9)
T76	160	188(3)	6,000	3(5)	-22 & 13(7)(10)	4.8W	18.4	1.52	4.2	36	.188	(9)
T77	158	154(3)	9,400	3(5)	0 & 18(7)(10)	0	23.3	1.76	5.1	27	.161	1.06
T78	158	154(3)	9,400	3(5)	-18 & 18(7)(10)	0	23.5	1.72	5.1	25	.161	.92
T79	159	155(3)	9,400	3(5)	-41 & 10(7)(10)	0	21.7	2.24	6.1	20	.161	.79
T80	158	155(3)	9,400	3(5)	-42 & 10(7)(10)	1.6W	21.5	2.24	5.5	22	.161	.81
T81	161	220(3)	7,800	3(5)	-51 & 0(7)(10)	0	27.4	1.92	6.8	24	.161	.81
T82	161	257(3)	6,900	3(5)	-55 & 0(7)(10)	0	26.1	2.76	7.8	27	.161	.89
T83	109	91Ar	1,950	4	0	0	2.5	1.4(11)		18	.140	.57
T84	162	131(3)	13,200	4	0	0	25.3	6.0(11)		35	.140	1.23
T85	162	128(3)	12,700	4	0	0	25.7	5.2(11)		34	.140	1.14
T86	162	185(1)	98,000(2)	3(5)	11Ar	0	8.3	1.40	4.8	34	.140	1.45
T87	164	135(1)	144,700(2)	3(5)	11Ar	.51W	14.9	1.40	5.0	34	.140	1.49
T88	161	185(1)	152,000(2)	3(5)	11Ar	.49W	16.2	1.44	4.8	37	.140	1.48
T89	163	121(3)	12,300	3(5)	14	0	24.5	1.18	5.82	39	.140	1.40
T90	162	121(3)	12,100	3(5)	14	.49W	24.9	1.15	5.66	38	.140	1.37
T91	161	121(3)	12,400	3(5)	14	.53W	25.4	1.10	5.30	38	.140	1.33
T92	157	152(1)	148,000(2)	3(5)	13	0	11.3	1.37	5.08	27	.140	1.28
T93	159	148(1)	127,000(2)	3(5)	13	0.01Si	8.4	1.33	4.97	29	.140	1.39
T94	160	152(1)	116,000(2)	3(5)	13	1.62Si	7.5	1.36	4.80	34(12)	.140	1.48
T96	81	113Ar	1,300	5	62(3) & 310(7)	4.8W	-	-	-	18	.140	1.12
T97	145	138(3)	10,900	5	77(3) & 368(7)	12.6W	-	-	-	31.0	.140	2.06

(1) H_2-Ar Mixture (2) For H_2 Gas (3) Air (4) Nitrogen (5) No Permeable Inserts (6) With Optional Inserts (7) Flow Listed for Plenum & Nozzle Inserts Respectively (8) Decreasing Due to Throat Erosion (9) Erratic Data Due to Gas Bleed Off (10) Negative Number Indicates Bleed Off (11) Single Piece Nozzle Insert (12) Pressure Increasing due to Accumulation of Seeding Material

TABLE II

MEASURED AND CALCULATED THRUSTS

Run No.*	Measured Thrust	Calculated Thrust	
		Coaxial Flow	Wind Tunnel Technique
T-46	1.30	1.14	1.10
T-48	1.28	1.07	1.17
T-49	1.70	1.44	1.27
T-52	1.71	1.53	1.26

*See Table I for detailed run conditions.

SPECIAL 5/8 DIA TORCH FOR HYDROGEN OPERATION

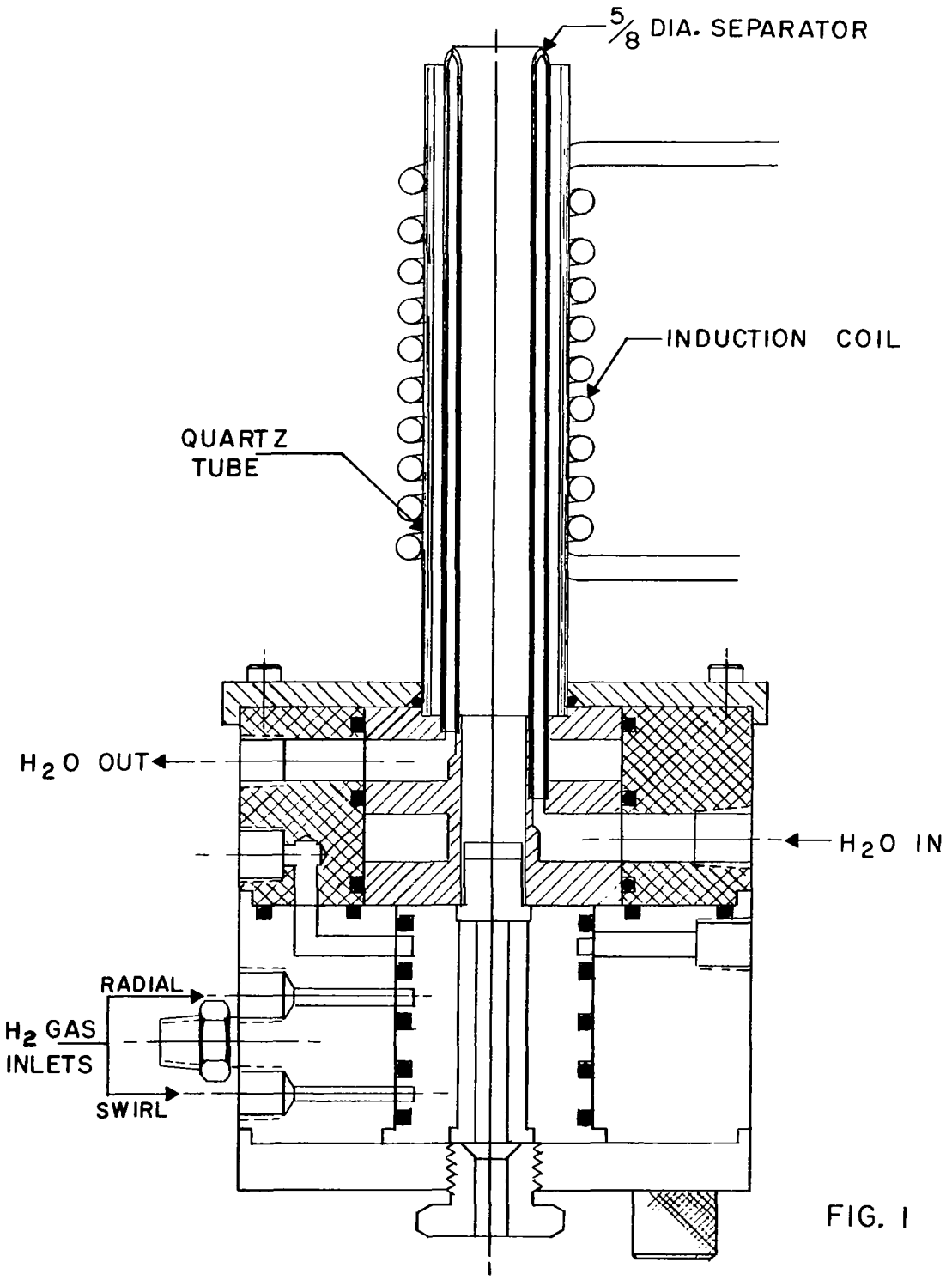

FIG. 1

ENERGY DISTRIBUTION IN AN INDUCTION PLASMA SYSTEM

(STEEL CALORIMETER, 3" TUBE MODEL 66 TORCH)

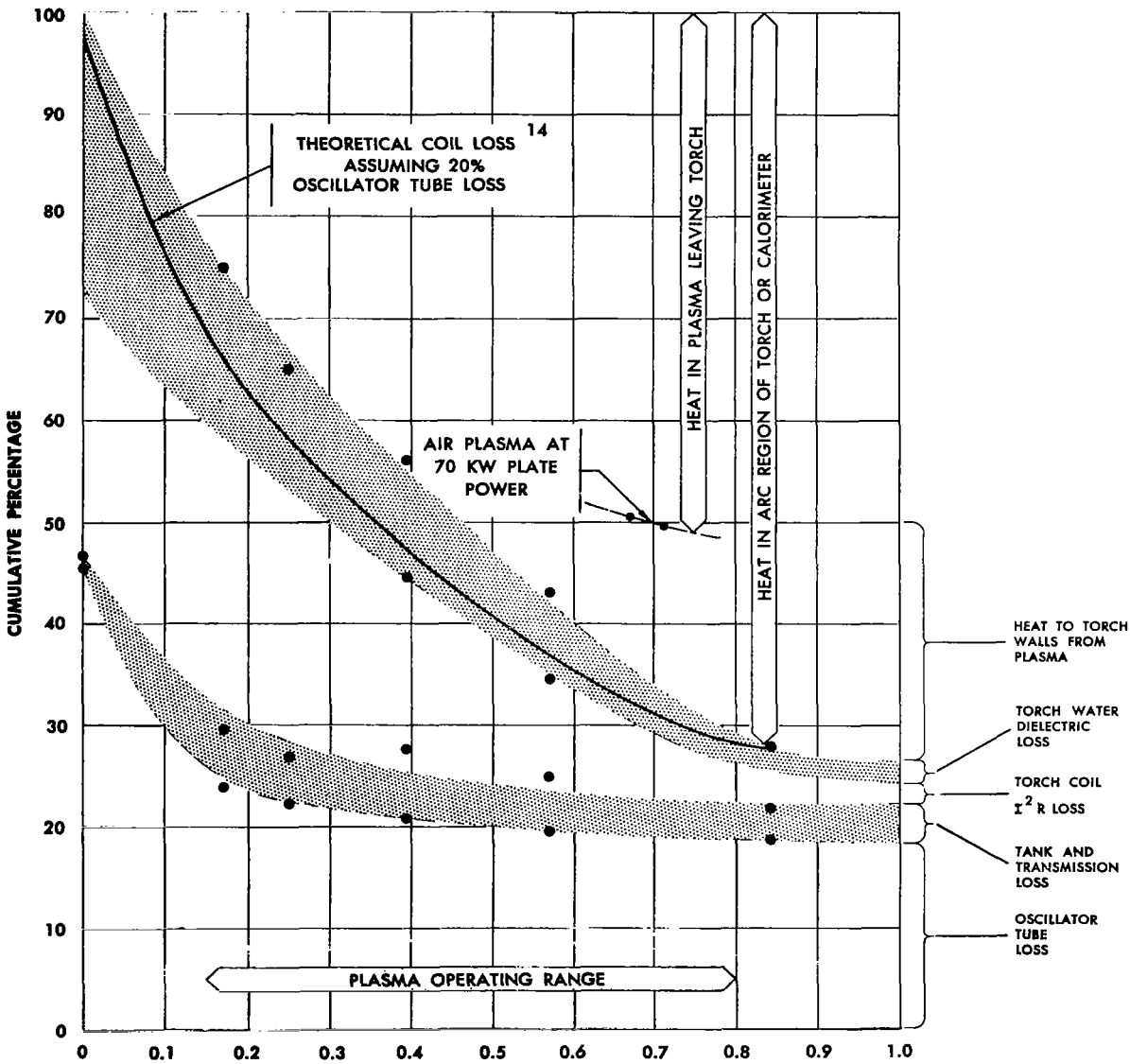

FIG. 2

EQUIPMENT SET-UP FOR SOLID VAPORIZATION FROM A CRUCIBLE

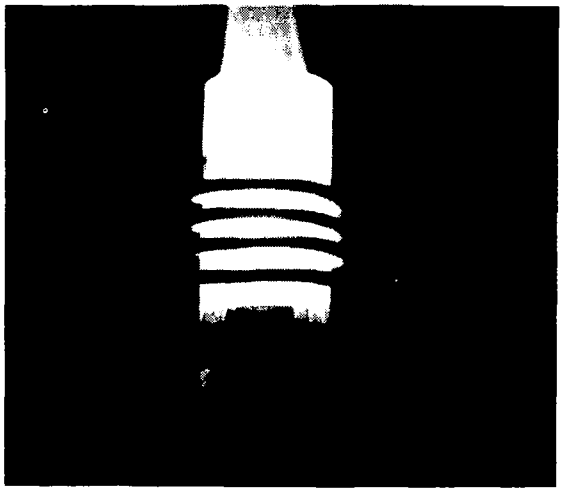

OPERATION WITH SODIUM CHLORIDE IN CRUCIBLE

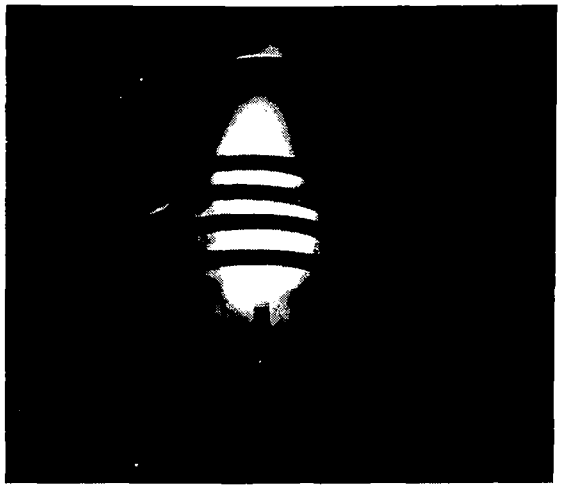

OPERATION WITH ZINC METAL WIRE FEED

FIG. 3

INDUCTION AUGMENTED DC PLASMA

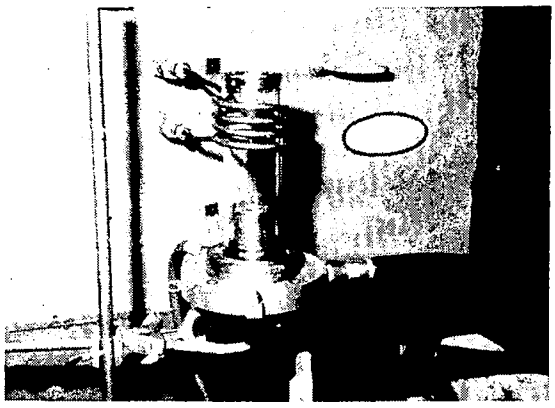

(A) EQUIPMENT SET-UP

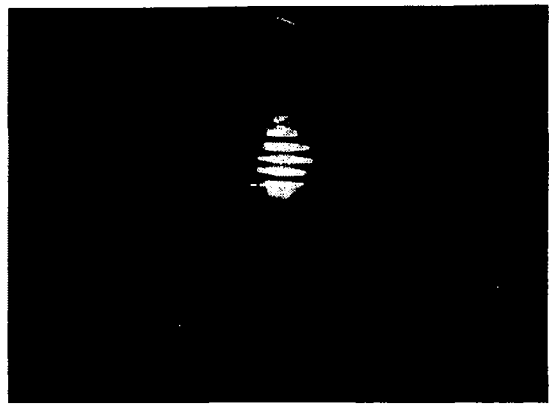

(C) RF OPERATION ONLY

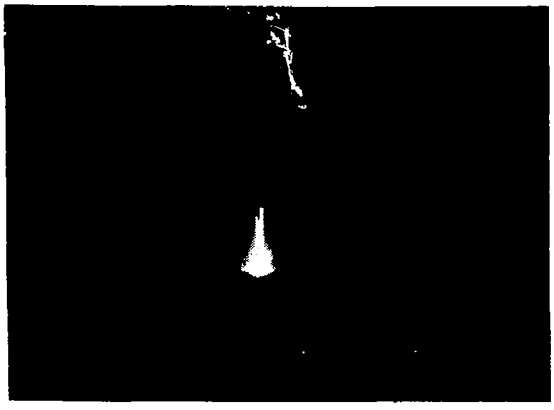

(B) DC OPERATION ONLY

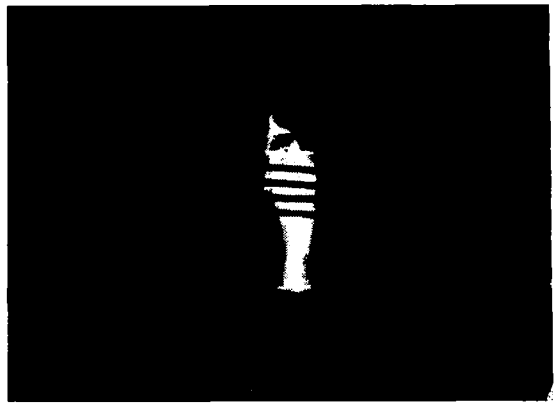

(D) RF AUGMENTED DC OPERATION

FIG. 4

INITIAL SEGMENTED NOZZLE DESIGN

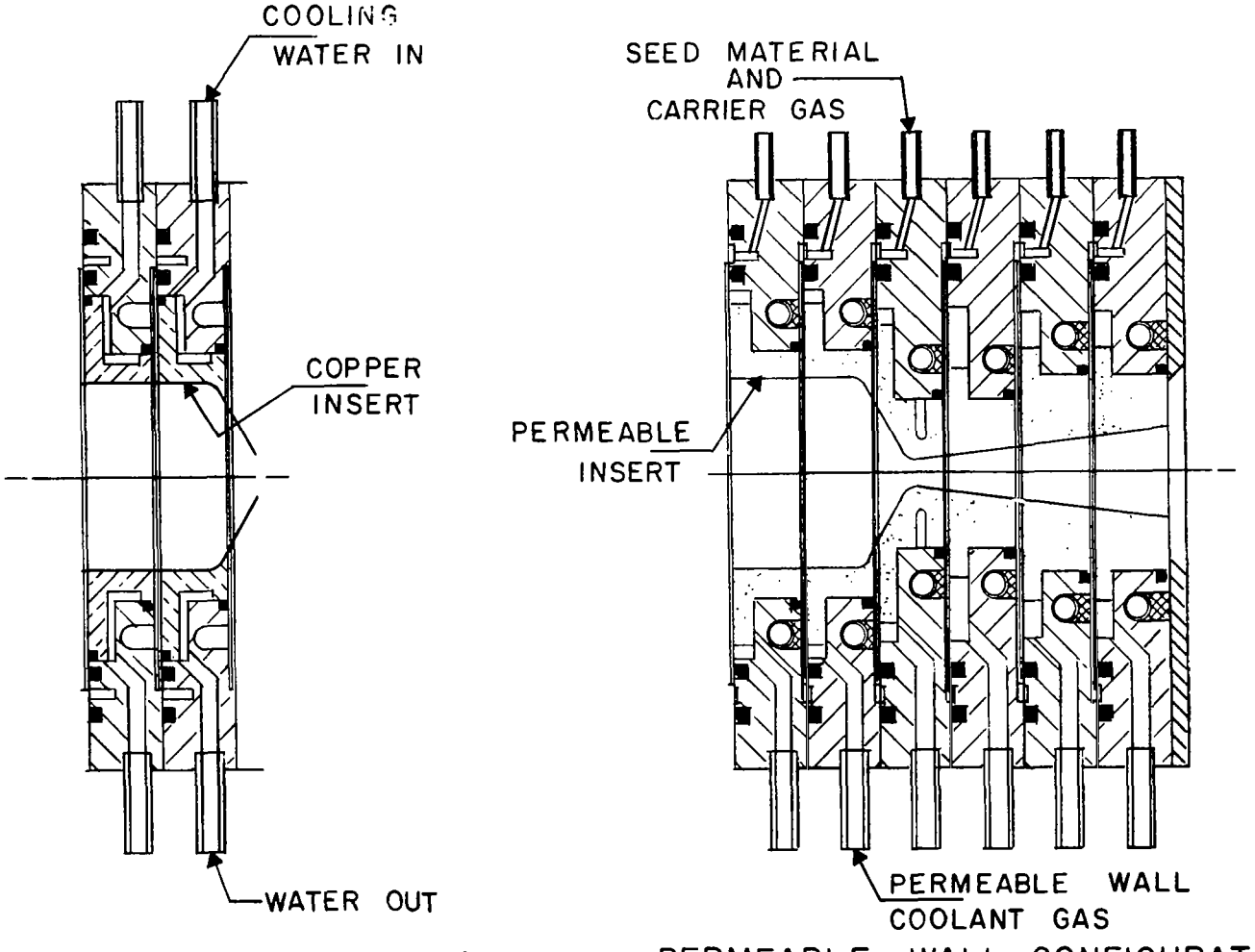

SOLID WALL CONFIGURATION

PERMEABLE WALL CONFIGURATION

FIG. 5

#1 NOZZLE CONFIGURATION

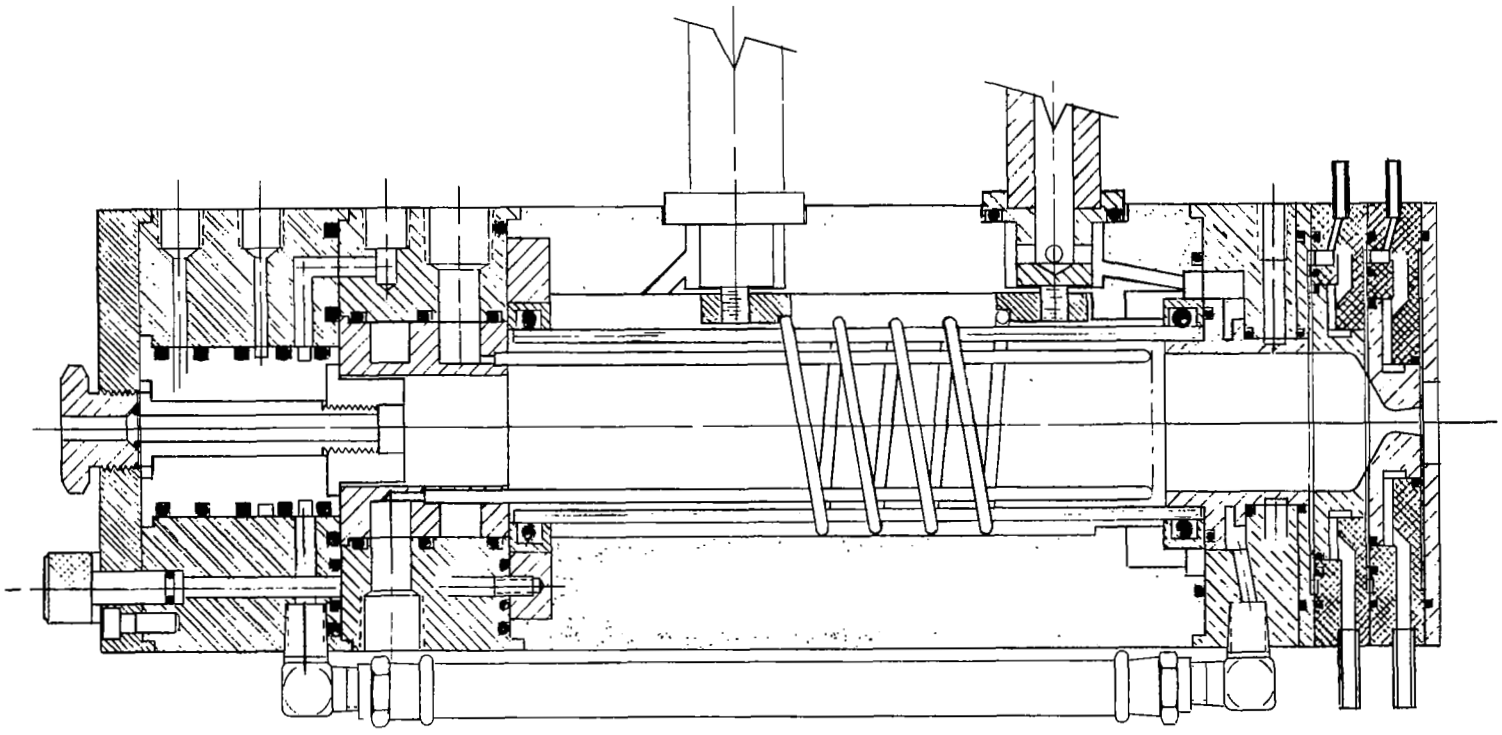

MODIFIED MODEL 56 TORCH
COPPER INSERTS FOR
CALORIMETRY STUDIES

FIG. 6

#2 NOZZLE CONFIGURATION

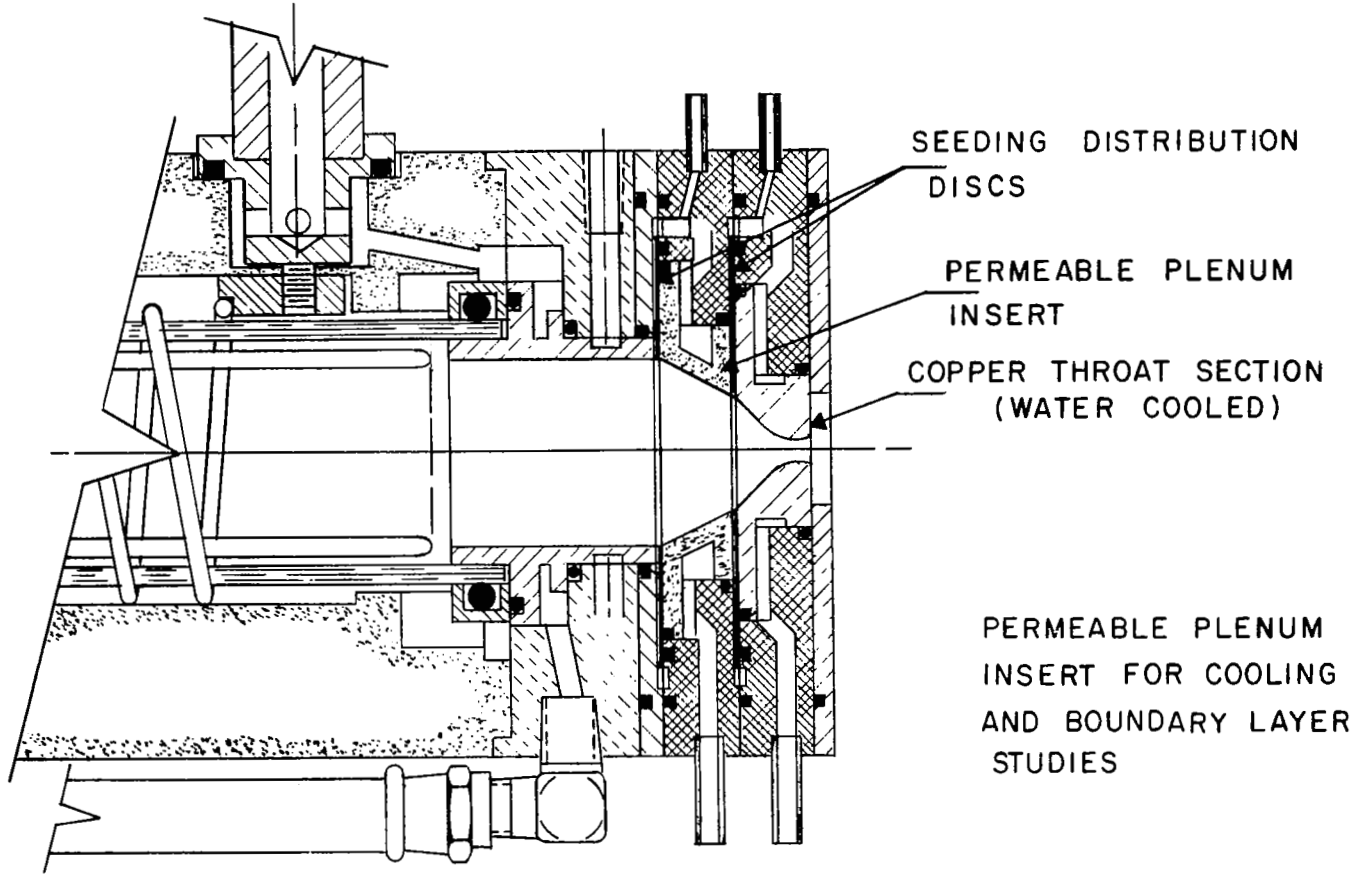

FIG. 7

#3 NOZZLE CONFIGURATION

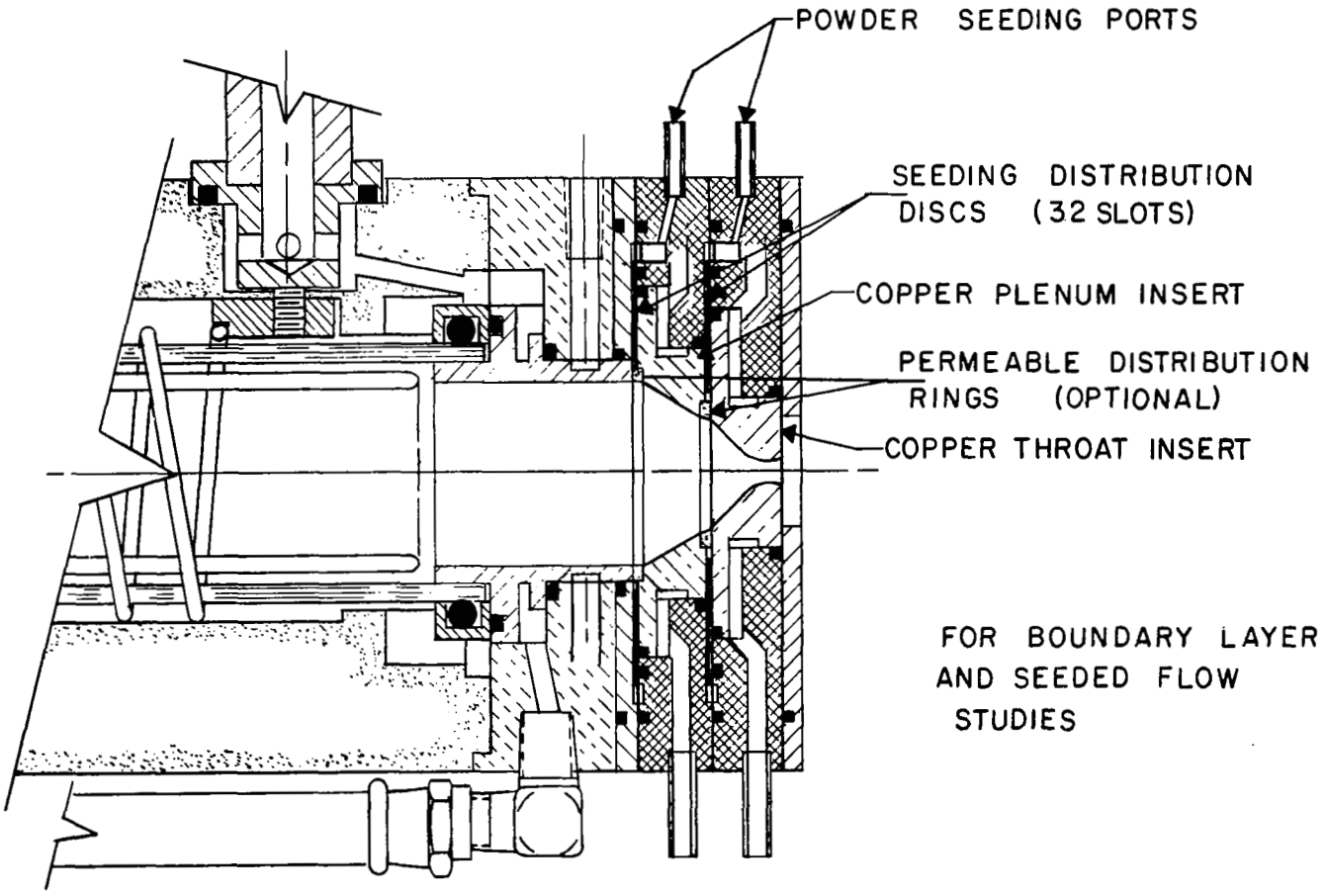

FIG. 8

#4 NOZZLE CONFIGURATION

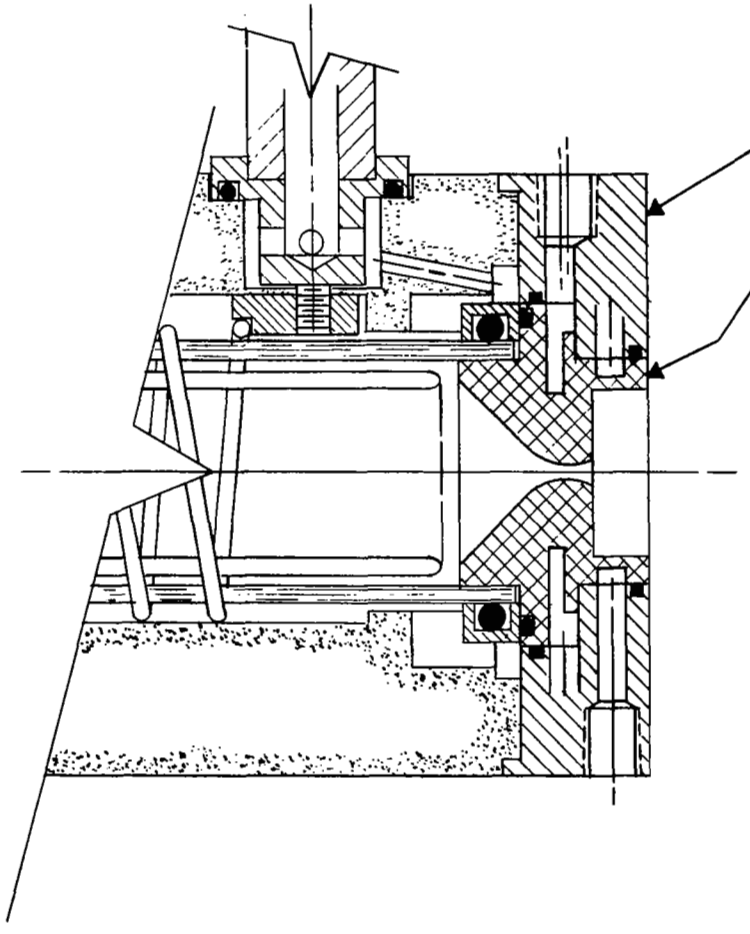

FIG. 9

#5 NOZZLE CONFIGURATION

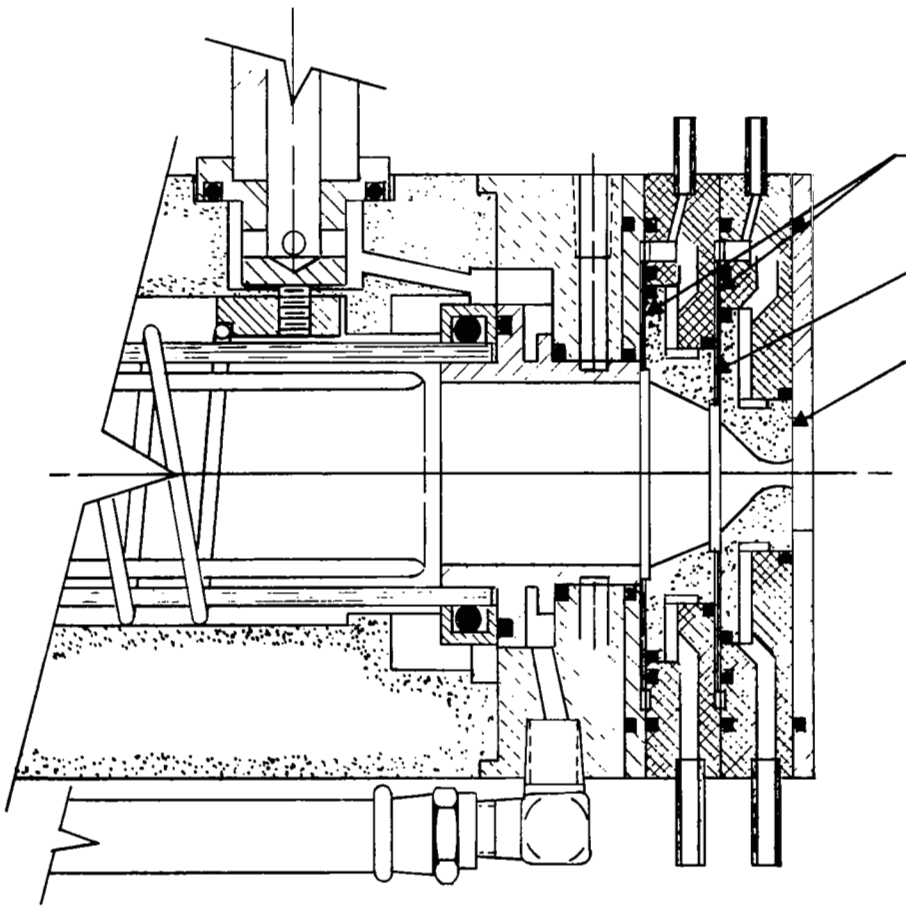

PERMEABLE GRAPHITE PLENUM AND THROAT INSERTS FOR TRANSPIRATION COOLING AND SEEDED FLOW STUDIES

FIG. 10

SCHEMATIC FOR LOAD CELL THRUST MEASUREMENT SYSTEM

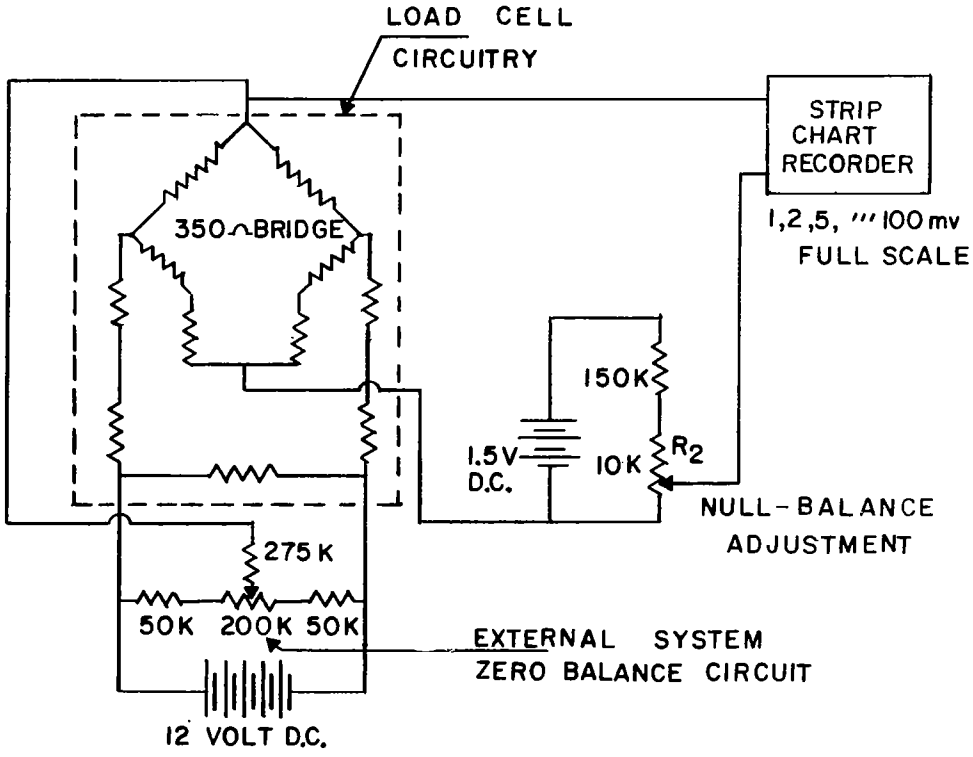

FIG. 11

LOAD CELL THRUST MEASURING SET-UP

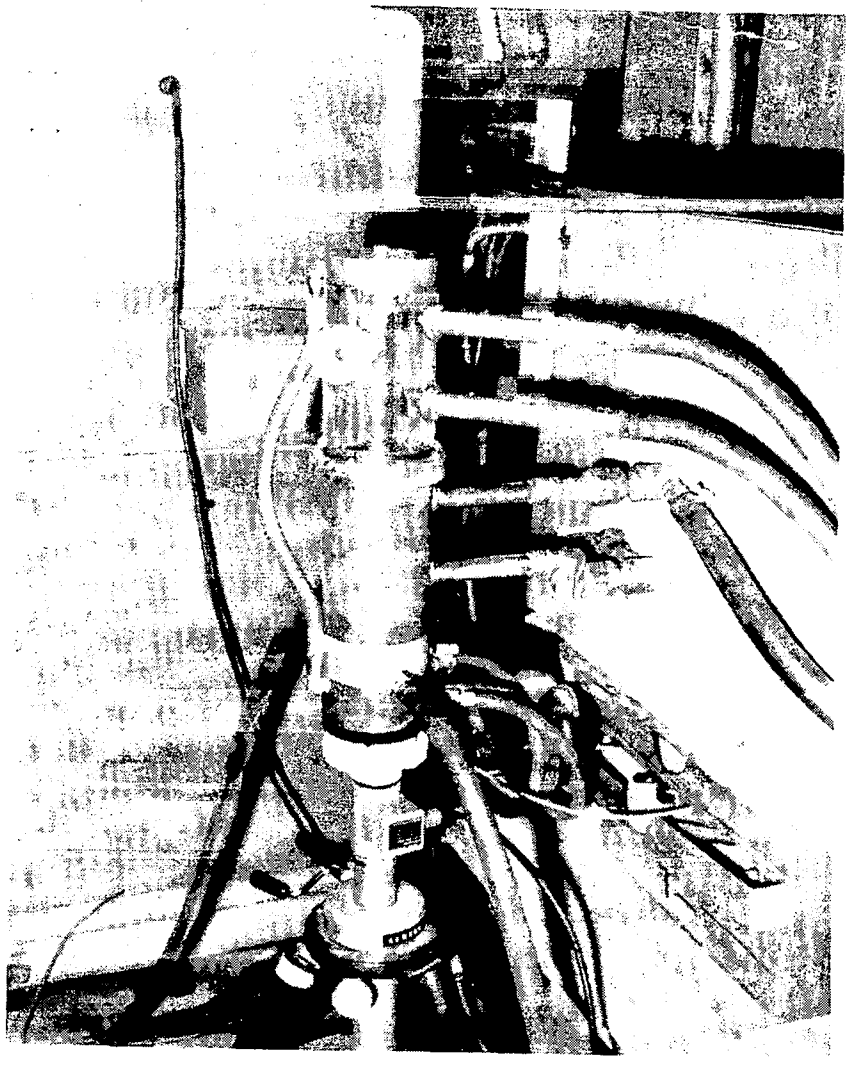

FIG. 12

MECHANICAL THRUST MEASURING SYSTEM

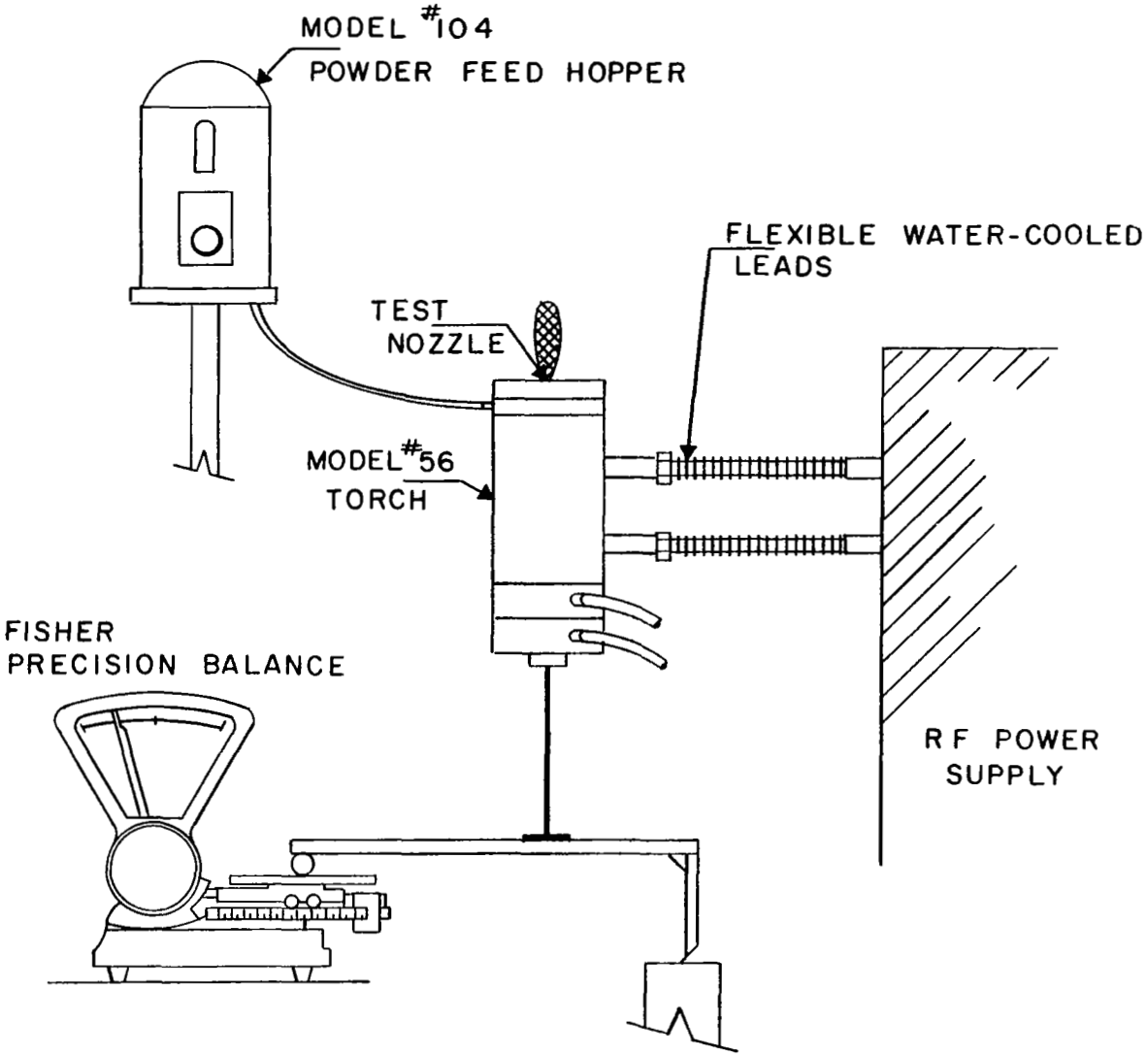

FIG. 13

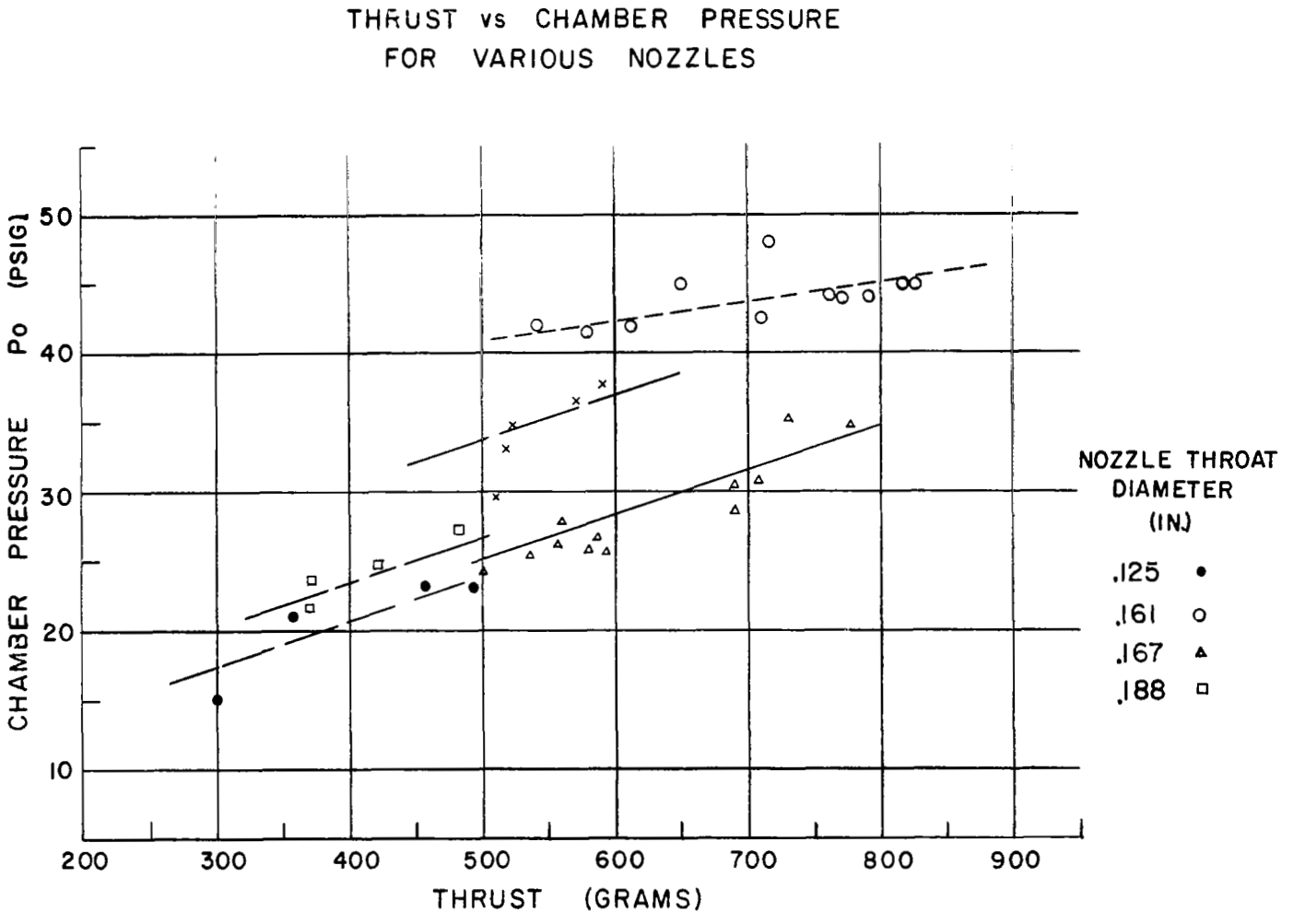
THRUST vs CHAMBER PRESSURE
FOR VARIOUS NOZZLES
CHAMBER PRESSURE Po (PSIG)
50
40
30
20
10
200
300
400
500
600
700
800
900
THRUST (GRAMS)
NOZZLE THROAT DIAMETER (IN.)
.125
.161
.167
.188

FIG. 14

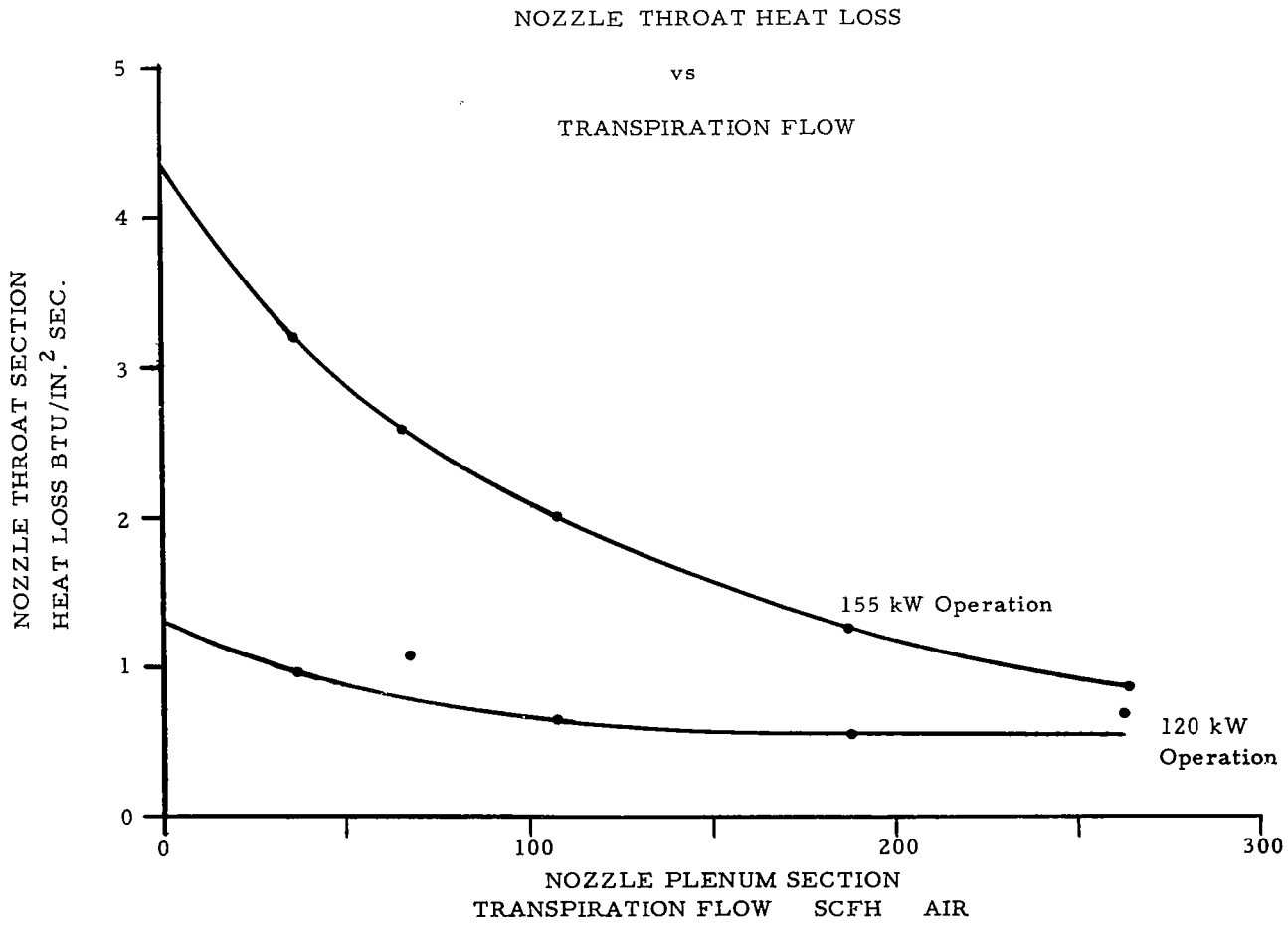
NOZZLE THROAT HEAT LOSS
vs
TRANSPIRATION FLOW
NOZZLE THROAT SECTION
HEAT LOSS BTU/IN.2 SEC.
5
4
3
2
1
0
155 kW Operation
120 kW
Operation
0
100
200
300
NOZZLE PLENUM SECTION
TRANSPIRATION FLOW SCFH AIR

FIG. 15

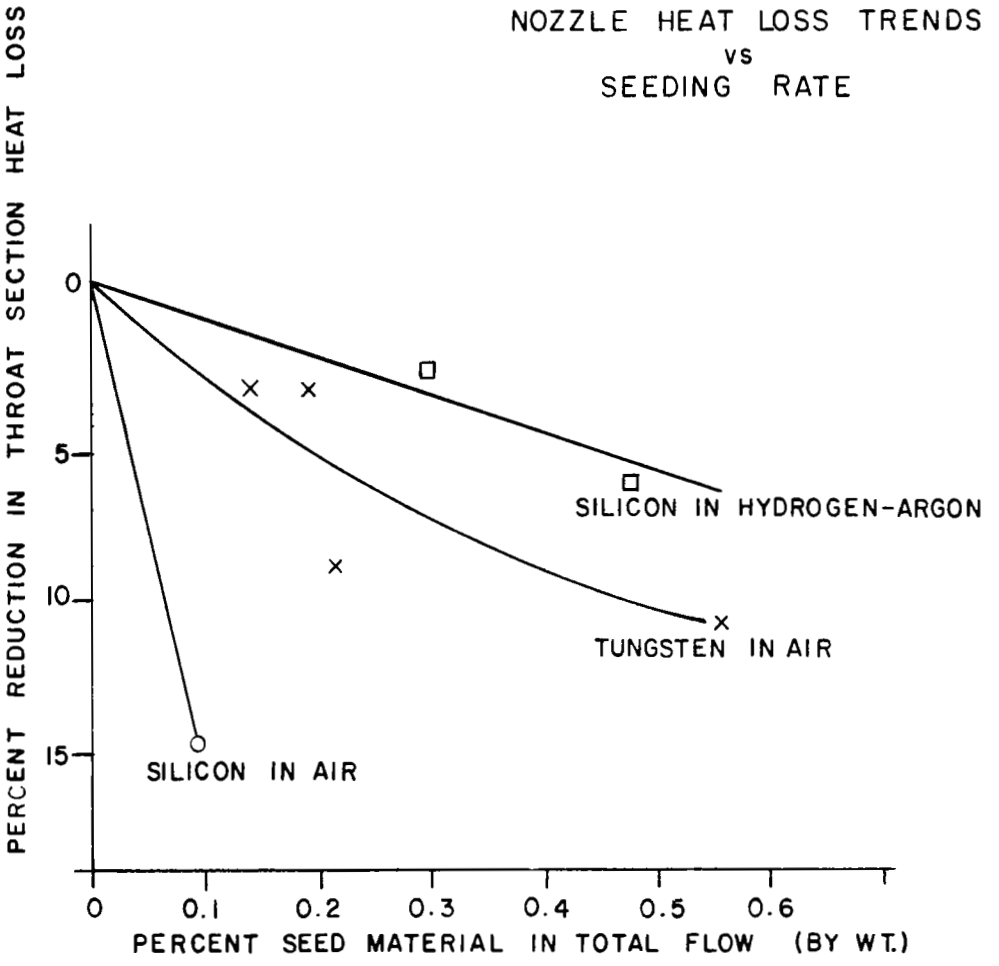

ZERO SEEDING NOZZLE HEATING RATES (BTU/IN^2 SEC.)	
Si IN H_2—Ar	5.1
W IN AIR	5.8
Si IN AIR	1.6

FIG. 16

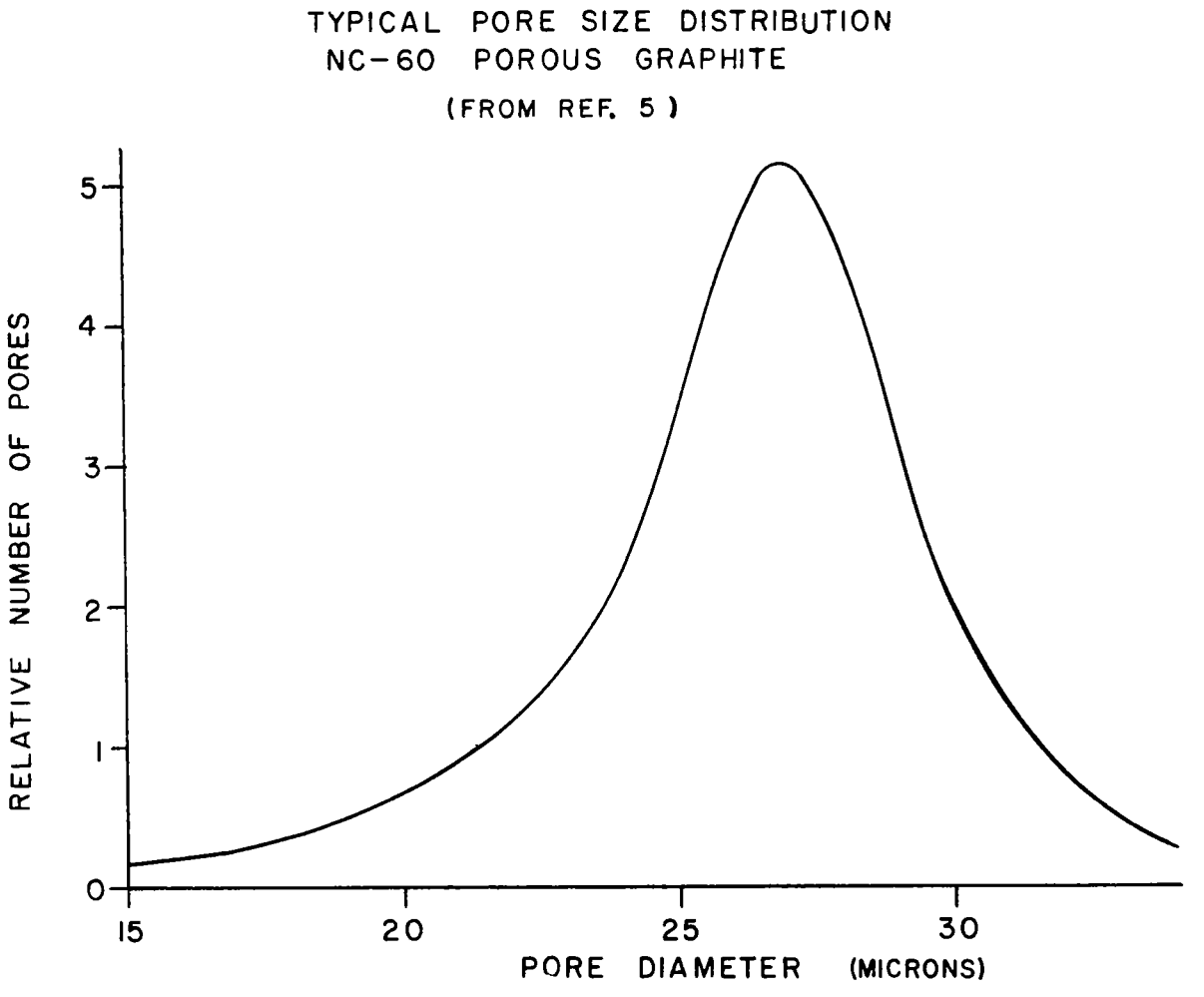
TYPICAL PORE SIZE DISTRIBUTION
NC-60 POROUS GRAPHITE
(FROM REF. 5)
RELATIVE NUMBER OF PORES
0
1
2
3
4
5
15
20
25
30
PORE DIAMETER (MICRONS)

FIG. 17

TYPICAL COLD FLOW PROFILE FOR
NC-60 POROUS GRAPHITE
(FROM REF. 5)

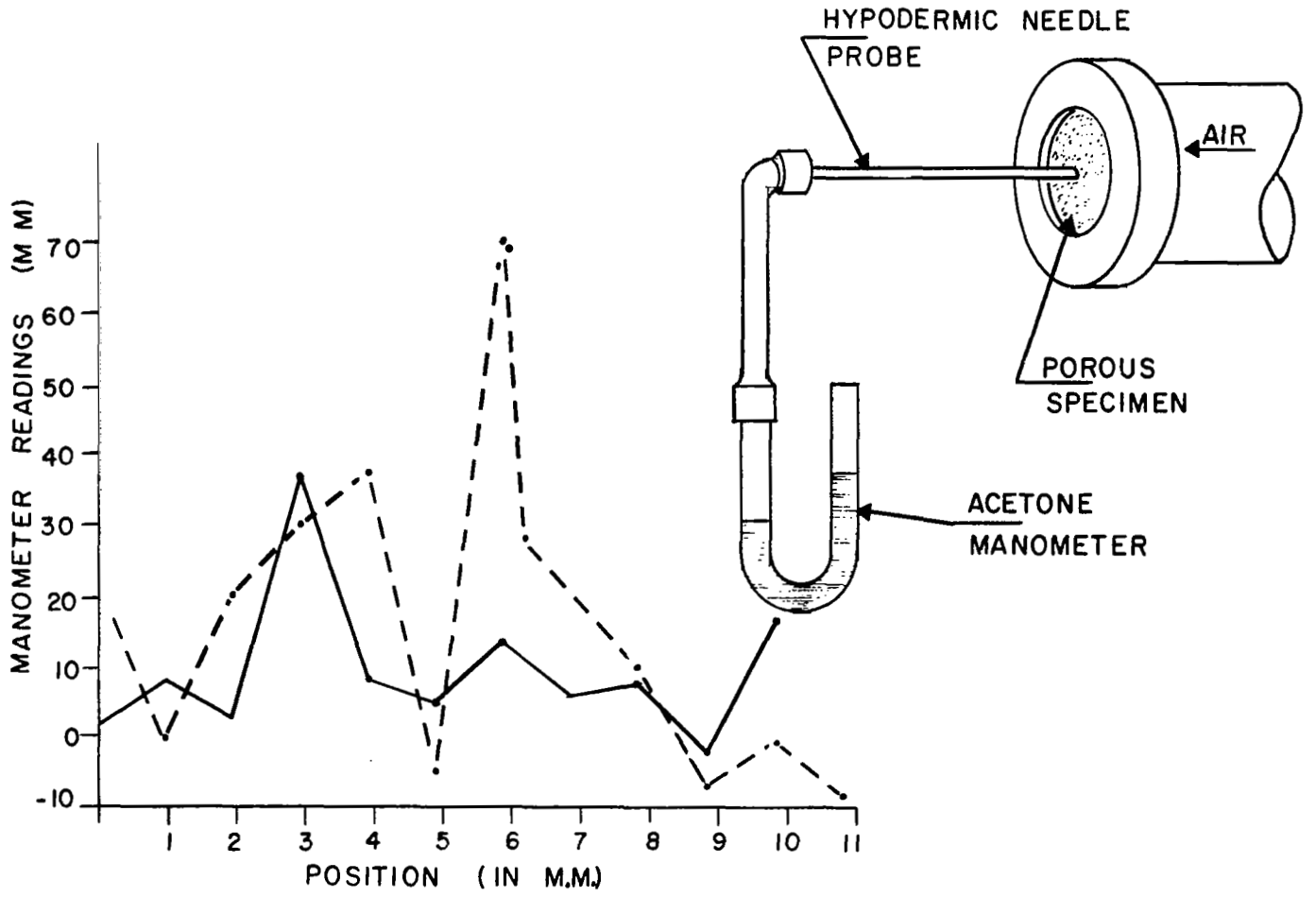

FIG. 18

VARIATION OF WEIGHT-FLOW AT THROAT
WITH STAGNATION ENTHALPY
(FROM REF. 6)

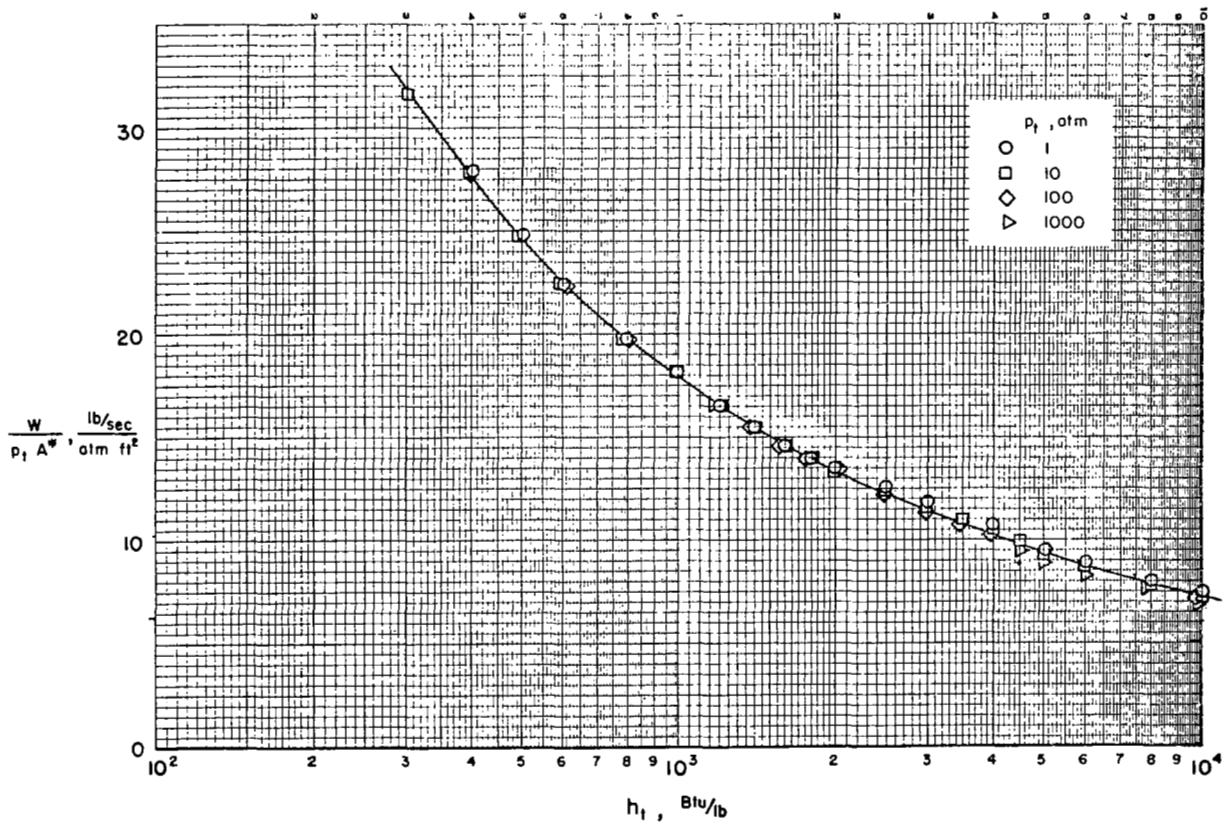

FIG. 19

VARIATION OF VELOCITY WITH MACH NUMBER
(FROM REF. 9)

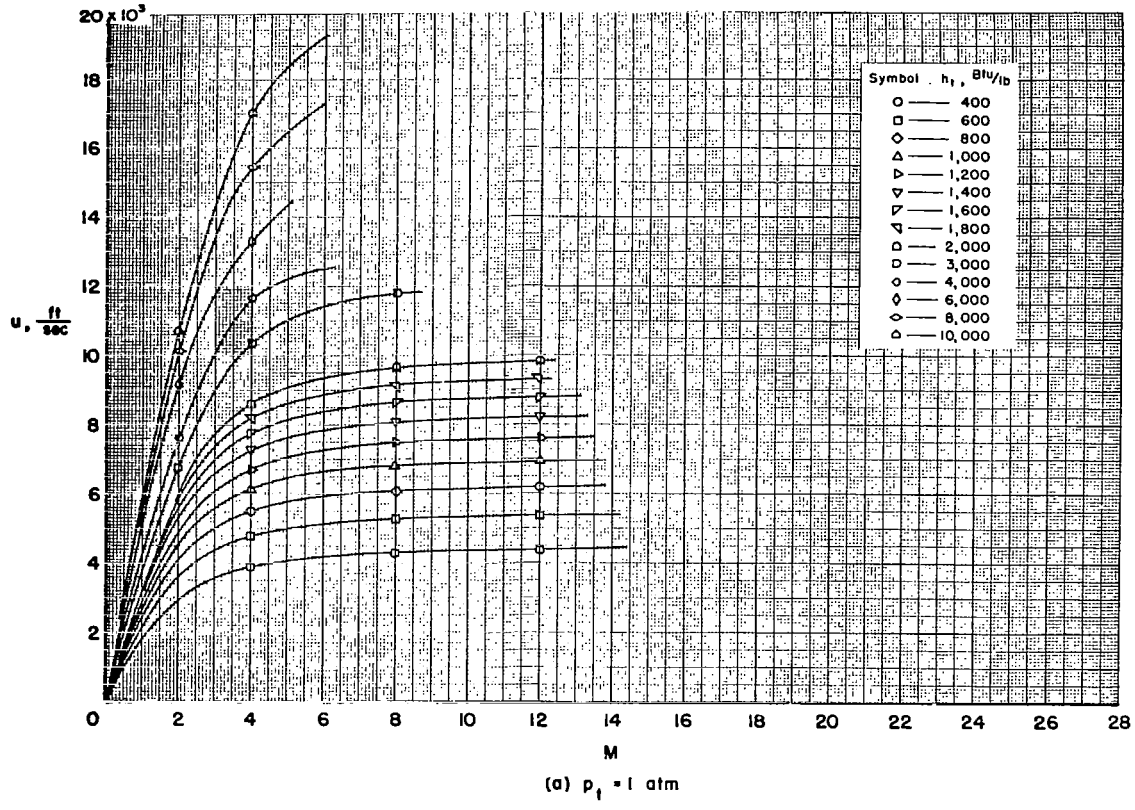

FIG. 20

THERMODYNAMIC CHARTS FOR AIR
(FROM REF. 10)

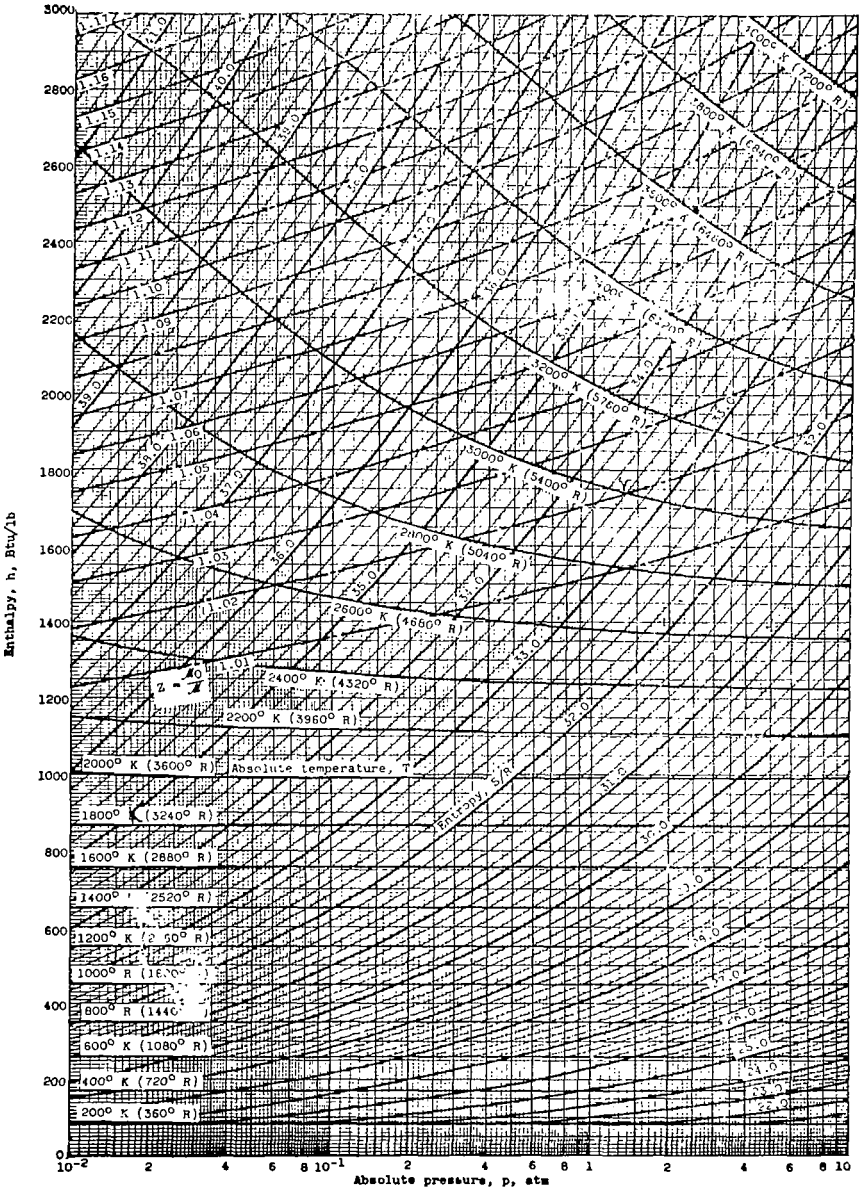

FIG. 21

ISENTROPIC EXPONENT FOR AIR IN EQUILIBRIUM
(FROM REF. 11)

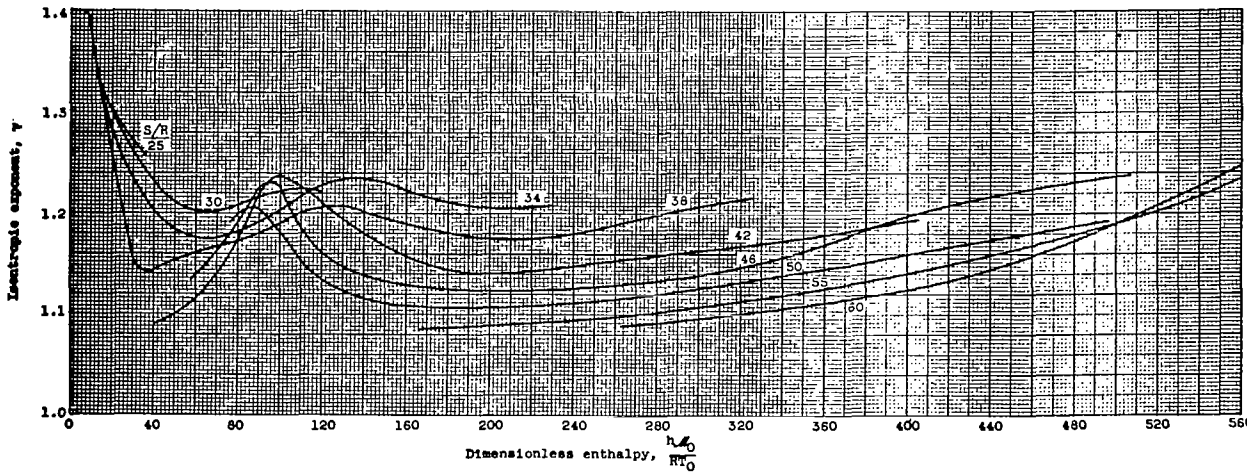

FIG. 22